

# Shear viscosity in neutron star cores

P. S. Shternin and D. G. Yakovlev

*Ioffe Physical Technical Institute, Politekhnicheskaya 26, 194021 Saint-Petersburg, Russia*

(Dated: May 26, 2019)

We calculate the shear viscosity  $\eta \approx \eta_{e\mu} + \eta_n$  in a neutron star core composed of nucleons, electrons and muons ( $\eta_{e\mu}$  being the electron-muon viscosity, mediated by collisions of electrons and muons with charged particles, and  $\eta_n$  the neutron viscosity, mediated by neutron-neutron and neutron-proton collisions). Deriving  $\eta_{e\mu}$ , we take into account the Landau damping in collisions of electrons and muons with charged particles via the exchange of transverse plasmons. It lowers  $\eta_{e\mu}$  and leads to the non-standard temperature behavior  $\eta_{e\mu} \propto T^{-5/3}$ . The viscosity  $\eta_n$  is calculated taking into account that in-medium effects modify nucleon effective masses in dense matter. Both viscosities,  $\eta_{e\mu}$  and  $\eta_n$ , can be important, and both are calculated including the effects of proton superfluidity. They are presented in the form valid for any equation of state of nucleon dense matter. We analyze the density and temperature dependence of  $\eta$  for different equations of state in neutron star cores, and compare  $\eta$  with the bulk viscosity in the core and with the shear viscosity in the crust.

PACS numbers: 97.60.Jd, 52.25.Fi, 52.27.Ny

## I. INTRODUCTION

Neutron stars are very compact. Their typical masses are  $\sim 1.4 M_\odot$  (where  $M_\odot$  is the mass of the Sun), while their radii are as small as  $\sim 10$  km. As a result, a neutron star core contains matter, whose density  $\rho$  reaches several  $\rho_0$  ( $\rho_0 \approx 2.8 \times 10^{14}$  g cm $^{-3}$  being the density of the standard saturated nuclear matter). The core is composed of uniform neutron-rich nuclear matter and extends from  $\rho \approx 0.5 \rho_0$  to the stellar center (where  $\rho$  can be as high as  $10\rho_0$ ). It attracts special attention because of its poorly known composition and equation of state (EOS); e.g., Ref. [1]. From outside, the core is surrounded by a thin ( $\sim 1$  km thick) and light (a few per cent by mass) crust composed of atomic nuclei, strongly degenerate electrons and (after the neutron drip at  $\rho \gtrsim 4 \times 10^{11}$  g cm $^{-3}$ ) free neutrons.

In this paper, we study the shear viscosity of neutron star cores. It is an important transport property which affects the relaxation of hydrodynamic motions, particularly, a possible differential rotation within the star and stellar oscillations [2]. The shear viscosity can be important for damping gravitational wave driven instabilities (for instance, r-modes; e.g., [3] and references therein). Its knowledge is required to analyze the efficiency of such instabilities for generating gravitational waves.

For simplicity, we consider the cores composed of strongly degenerate neutrons (n), protons (p), electrons (e), and muons ( $\mu$ ) – npe $\mu$  matter, neglecting a possible appearance of hyperons and/or exotic forms of matter (pion or kaon condensates or quarks or their mixtures) as predicted by some EOSs at  $\rho \gtrsim 2\rho_0$ ; see, e.g., Ref. [1]. The electrons and muons constitute almost ideal gases. The muons are absent in the outermost part of the core. They appear at densities exceeding a threshold value  $\rho_\mu \sim \rho_0$  [4] at which the electron chemical potential reaches the muon rest-mass energy ( $\mu_e = m_\mu c^2 \approx 207 m_e c^2$ ). The electrons are ultra-relativistic, while the muons are non-relativistic just after the threshold but become relativistic at higher  $\rho$ . In contrast to electrons and muons, nucleons constitute a strongly interacting Fermi liquid where protons are essentially non-relativistic, while neutrons become mildly relativistic at  $\rho \gtrsim 2\rho_0$ . The neutrons and protons can be in superfluid state (e.g., Ref. [5]).

The main contribution to the shear viscosity  $\eta$  in a neutron star core comes from electrons and muons (lightest and most mobile particles) and neutrons (most abundant particles),

$$\eta = \eta_{e\mu} + \eta_n. \quad (1)$$

The viscosity  $\eta_{e\mu}$  of electrons and muons is mainly limited by collisions of electrons and muons between themselves and with other charged particles (protons, in our case) via electromagnetic forces. In contrast, the neutron contribution  $\eta_n$  is limited by neutron-neutron and neutron-proton collisions mediated by strong interactions. As a result,  $\eta_{e\mu}$  and  $\eta_n$  are nearly independent (belong to different – electromagnetic and nuclear – sectors) and can be calculated separately [6].

In applications, one often employs the viscosity  $\eta_{e\mu}$  calculated by Flowers and Itoh [6] for non-superfluid matter. Recently, Andersson et al. [7] have estimated  $\eta_{e\mu}$  for superfluid matter. However, these studies neglect an enhancement of collisions of relativistic charged particles due to the exchange of transverse plasmons. The significance of this effect was demonstrated by Heiselberg and Pethick [8] in their study of transport properties of ultra-relativistic quark matter. Recently we (Shternin and Yakovlev [9] – hereafter SY07) have reconsidered the electron-muon thermal conductivity  $\kappa_{e\mu}$  taking into account the exchange of transverse plasmons. This effect can reduce  $\kappa_{e\mu}$  by several orders of magnitude.

Here we reanalyze  $\eta_{e\mu}$  in the same manner. We closely follow SY07 and omit technical details. In addition, we reconsider  $\eta_n$ , which is a more difficult task involving nucleon-nucleon collisions. The viscosity  $\eta_n$  was calculated by Flowers and Itoh [6] for one EOS of non-superfluid matter assuming in-vacuum nucleon-nucleon scattering. These results were fitted by Cutler and Lindblom [2] by a simple analytical expression which is widely used; according to Ref. [6],  $\eta_n > \eta_{e\mu}$ . Recently Benhar and Valli [10] have calculated  $\eta_n$  for pure neutron matter in a self-consistent manner using the same nucleon interaction potential to derive  $\eta_n$  and construct the EOS (also for one EOS). We calculate  $\eta_n$  in a more general way than Flowers and Itoh [6]. Our approach is similar to that used by Baiko, Haensel and Yakovlev [11] (hereafter BHY01) for evaluating the thermal conductivity of neutrons. In addition, we employ recent developments [12] in calculations of nucleon-nucleon scattering cross sections in nuclear matter. As in BHY01, we take into account superfluidity of protons. Again, we closely follow the derivation of BHY01 and omit the details.

After calculating  $\eta_{e\mu}$  and  $\eta_n$ , we analyze the shear viscosity in neutron star cores with different EOSs.

## II. SHEAR VISCOSITY IN NON-SUPERFLUID MATTER

The shear viscosity is calculated from a system of coupled Boltzmann kinetic equations

$$\mathbf{v}_c \frac{\partial F_c}{\partial \mathbf{r}} = \sum_i I_{ci}, \quad (2)$$

where  $F_c$  is the distribution function of momentum-transfer carriers  $c$  (with  $c = e, \mu$ , or  $n$ , in our case);  $i = n, p, e, \mu$  runs over all particle species;  $\mathbf{v}_c$  is the velocity of particles  $c$ , and  $I_{ci}$  is a collision integral, that describes a scattering of particles  $c$  and  $i$ :

$$I_{ci} = \frac{1}{(2\pi\hbar)^9(1+\delta_{ci})} \sum_{\sigma_1, \sigma_2, \sigma_{2'}} \int d\mathbf{p}_2 d\mathbf{p}_{1'} d\mathbf{p}_{2'} w_{ci}(12|1'2') \\ \times [F_{1'}F_{2'}(1-F_1)(1-F_2) - F_1F_2(1-F_{1'})(1-F_{2'})]. \quad (3)$$

Here, 1 and 2 denote particle states before a collision; 1' and 2' are particle states after the collision;  $\mathbf{p}$  is the particle momentum,  $\sigma$  is the spin state, and  $w_{ci}$  is the differential transition probability. The Kronecker delta  $\delta_{ci}$  is included to avoid double counting of collisions between identical particles ( $c = i$ ).

Distributions  $F_c$  slightly deviate from the equilibrium Fermi-Dirac distributions  $f_c$  owing to the presence of a small hydrodynamical velocity field  $\mathbf{V}$ ,

$$F_c = f_c - \Phi_c \frac{\partial f_c}{\partial \varepsilon_c}, \quad f_c = \left\{ \exp \left( \frac{\varepsilon_c - \mu_c}{k_B T} \right) + 1 \right\}^{-1}, \quad (4)$$

where  $\varepsilon_c$  is the particle energy,  $\mu_c$  is its chemical potential,  $T$  is the temperature,  $k_B$  is the Boltzmann constant, and  $\Phi_c$  measures a deviation from equilibrium. The electron-muon and neutron transports are decoupled because we neglect electromagnetic interaction between the leptons and neutrons. For calculating  $\eta_{e\mu}$ , the electrons and muons are treated as the only momentum carriers which undergo collisions between themselves and with protons. For calculating  $\eta_n$ , the only momentum carriers are assumed to be neutrons, while the contribution of protons is neglected due to their small fraction. Therefore, the protons are thought to be passive scatterers which obey the equilibrium Fermi-Dirac distribution. Nonequilibrium parts of the electron, muon, and neutron distributions are found using the standard variational approach with the simplest trial function,

$$\Phi_c = -\tau_c \left( v_{c\alpha} p_{c\beta} - \frac{1}{3} v_c p_c \delta_{\alpha\beta} \right) V_{\alpha\beta}, \quad (5)$$

where  $\tau_c$  is an effective relaxation time of particles  $c$ ,  $\mathbf{v}_c$  is their velocity, and

$$V_{\alpha\beta} = \frac{1}{2} \left( \frac{\partial V_\alpha}{\partial x_\beta} + \frac{\partial V_\beta}{\partial x_\alpha} \right), \quad (6)$$

with  $\sum_\alpha V_{\alpha\alpha} = \text{div} \mathbf{V} = 0$ .

The resulting shear viscosity is expressed through the effective relaxation times in a standard way,

$$\eta = \eta_{e\mu} + \eta_n = \eta_e + \eta_\mu + \eta_n, \quad \eta_e = \frac{n_e p_{Fe}^2 \tau_e}{5m_e^*}, \quad \eta_\mu = \frac{n_\mu p_{F\mu}^2 \tau_\mu}{5m_\mu^*}, \quad \eta_n = \frac{n_n p_{Fn}^2 \tau_n}{5m_n^*}, \quad (7)$$

where  $\eta_e$ ,  $\eta_\mu$ , and  $\eta_n$  are, respectively, the partial electron, muon, and neutron shear viscosities;  $n_c$  is the number density of particles  $c$ ;  $p_{Fc}$  is their Fermi momentum; and  $m_c^*$  is an effective mass on their Fermi surface. The electron and muon effective masses differ from their rest masses due to relativistic effects,  $m_e^* = \mu_e/c^2$  and  $m_\mu^* = \mu_\mu/c^2$ . The neutron and proton effective masses differ from their bare masses mainly due to many-body effects in dense matter (being determined by neutron and proton densities of state near appropriate Fermi surfaces).

Linearizing the kinetic equations, multiplying them by  $(v_{1\alpha}p_{1\beta} - \frac{1}{3}v_1p_1\delta_{\alpha\beta})$ , summing over  $\sigma_1$  and integrating over  $(2\pi\hbar)^{-3}d\mathbf{p}_1$ , we obtain a system of equations for the relaxation times,

$$1 = \sum_i (\nu_{ci}\tau_c + \nu'_{ci}\tau_i), \quad c = e, \mu, n, \quad (8)$$

where we introduce the effective collision frequencies,

$$\begin{aligned} \nu_{ci} &= \frac{3\pi^2\hbar^3}{2p_{Fc}^5 k_B T m_c^*} \int \frac{d\mathbf{p}_1 d\mathbf{p}_{1'} d\mathbf{p}_2 d\mathbf{p}_{2'}}{(2\pi\hbar)^{12}} W_{ci}(12|1'2') f_1 f_2 (1-f_{1'}) (1-f_{2'}) \\ &\times \left[ \frac{2}{3} p_1^4 + \frac{1}{3} p_1^2 p_{1'}^2 - (\mathbf{p}_1 \cdot \mathbf{p}_{1'})^2 \right], \end{aligned} \quad (9)$$

$$\begin{aligned} \nu'_{ci} &= \frac{3\pi^2\hbar^3}{2p_{Fc}^5 k_B T m_i^*} \int \frac{d\mathbf{p}_1 d\mathbf{p}_{1'} d\mathbf{p}_2 d\mathbf{p}_{2'}}{(2\pi\hbar)^{12}} W_{ci}(12|1'2') f_1 f_2 (1-f_{1'}) (1-f_{2'}) \\ &\times \left[ \frac{1}{3} p_1^2 p_{2'}^2 - \frac{1}{3} p_1^2 p_2^2 + (\mathbf{p}_1 \cdot \mathbf{p}_2)^2 - (\mathbf{p}_1 \cdot \mathbf{p}_{2'})^2 \right], \end{aligned} \quad (10)$$

with  $W_{ci}(12|1'2') = (1 + \delta_{ci})^{-1} \sum_{\text{spins}} w_{ci}(12|1'2')$  (the sum is over spin states of all particles 1,2,1',2').

The formal solution of (8) for the npe $\mu$ -matter is

$$\tau_e = \frac{\nu_\mu - \nu'_{e\mu}}{\nu_e \nu_\mu - \nu'_{e\mu} \nu'_{\mu e}}, \quad \tau_\mu = \frac{\nu_e - \nu'_{\mu e}}{\nu_e \nu_\mu - \nu'_{e\mu} \nu'_{\mu e}}, \quad \tau_n = \frac{1}{\nu_n}, \quad (11)$$

where

$$\begin{aligned} \nu_e &= \sum_i \nu_{ei} + \nu'_{ee} = \nu_{ee} + \nu'_{ee} + \nu_{e\mu} + \nu_{ep}, \\ \nu_\mu &= \sum_i \nu_{\mu i} + \nu'_{\mu\mu} = \nu_{\mu\mu} + \nu'_{\mu\mu} + \nu_{\mu e} + \nu_{\mu p}, \\ \nu_n &= \nu_{nn} + \nu'_{nn} + \nu_{np}. \end{aligned} \quad (12)$$

In the absence of muons, the expression for  $\eta_{e\mu}$  simplifies,

$$\eta_{e\mu} = \eta_e, \quad \tau_e^{-1} = \nu_e = \nu_{ee} + \nu'_{ee} + \nu_{ep}. \quad (13)$$

Once collision frequencies are found, the viscosity is obtained from Eq. (7). In order to determine the collision frequencies from Eqs. (9) and (10) one needs to know the transition probability  $W_{ci}(12|1'2')$ . The collisions of charged particles should be considered with a proper treatment of plasma screening of electromagnetic interaction. We discuss the plasma screening and the calculation of  $\eta_{e\mu}$  in Secs. II A–II C. The neutron viscosity  $\eta_n$  is studied in Sec. II D. In Sec. II we consider nonsuperfluid nucleons; the effects of proton superfluidity are analyzed in Sec. III. Throughout the paper we use the simplest variational approach. A comparison with an exact solution is discussed in Sec. II C 4.

### A. Plasma screening

The plasma screening in neutron star cores is discussed in SY07. Here, we outline the main points. The differential collision probability can be written as

$$W_{ci}(12|1'2') = 4 \frac{(2\pi\hbar)^4}{\hbar^2} \delta(\mathbf{p}_1 + \mathbf{p}_2 - \mathbf{p}_{1'} - \mathbf{p}_{2'}) \delta(\varepsilon_1 + \varepsilon_2 - \varepsilon_{1'} - \varepsilon_{2'}) \frac{\langle |M_{ci}|^2 \rangle}{1 + \delta_{ci}}, \quad (14)$$

where  $\langle |M_{ci}|^2 \rangle$  is the squared matrix element summed over final and averaged over initial spin states. For collisions of identical particles, we have  $M_{cc} = M_{cc}^{(1)} - M_{cc}^{(2)}$ , where the first and second terms correspond to the scattering channels  $12 \rightarrow 1'2'$  and  $12 \rightarrow 2'1'$ , respectively. Collisions of different particles go through a single channel,  $M_{ci} = M_{ci}^{(1)}$ ,

$$M_{ci}^{(1)} = \frac{4\pi e^2}{c^2} \left( \frac{J_{1'1}^{(0)} J_{2'2}^{(0)}}{q^2 + \Pi_l} - \frac{\mathbf{J}_{t1'1} \cdot \mathbf{J}_{t2'2}}{q^2 - \omega^2/c^2 + \Pi_t} \right), \quad (15)$$

where  $\hbar \mathbf{q} = \mathbf{p}_{1'} - \mathbf{p}_1$  and  $\hbar \omega = \varepsilon_{1'} - \varepsilon_1$  are, respectively, momentum and energy transfers in a collision event;  $J_{c'c}^{(\nu)} = (J_{c'c}^{(0)}, \mathbf{J}_{c'c}) = (2m_c^* c)^{-1} (\bar{u}_{c'} \gamma^\nu u_c)$  is the transition 4-current ( $\nu = 0, 1, 2, 3$ ),  $\mathbf{J}_{t'c}$  is the component of  $\mathbf{J}_{c'c}$  transverse to  $\mathbf{q}$ ;  $\gamma^\nu$  is a Dirac matrix;  $u_c$  a normalized bispinor (with  $\bar{u}_c u_c = 2m_c c^2$ ), and  $\bar{u}_c$  is a Dirac conjugate. The first term in Eq. (15) corresponds to direct Coulomb interaction via the longitudinal currents (with respect to  $\mathbf{q}$ ); the space-like longitudinal component of the current is expressed through the time-like component  $J_{c'c}^{(0)}$  with the aid of charge conservation condition. The second term describes the interaction via transverse currents. It is especially important for relativistic particles because  $J_{c'c}/J_{c'c}^{(0)} \sim p_c/(m_c^* c)$ . Longitudinal and transverse interactions are accompanied by different plasma screenings described by the functions  $\Pi_t$  and  $\Pi_l$  in the denominators of Eq. (15).

The collision energy and momentum transfers in neutron star cores are typically small,  $\hbar \omega \sim k_B T \ll \varepsilon_i$  and  $\hbar q \ll p_{Fi}$ . This smallness allows us to use the weak-screening approximation which greatly simplifies the consideration. Moreover, one typically has  $\omega \ll q v_{Fi}$ , so that it is sufficient to use the asymptotic expressions (e.g., SY07)

$$\Pi_l = q_l^2 = \frac{4\alpha}{\pi \hbar^2} \sum_i m_i^* p_{Fi} c, \quad (16)$$

$$\Pi_t = i \frac{\pi}{4} \frac{\omega}{q c} q_t^2 = i \frac{\alpha}{\hbar^2} \frac{\omega}{q c} \sum_i p_{Fi}^2, \quad (17)$$

where  $\alpha = e^2/\hbar c \approx 1/137$  is the fine structure constant;  $q_l$  and  $q_t$  are characteristic plasma wavenumbers which depend on plasma composition (summation is over all types of charged particles);  $q_l$  is the familiar Thomas-Fermi screening wavenumber;  $q_t \lesssim q_l$ , with  $q_t \rightarrow q_l$  in the limit of ultra-relativistic particles. Longitudinal interactions (via the exchange of longitudinal plasmons) are mediated by static non-dissipative screening with characteristic wavenumber  $q_l$  ( $\Pi_l$  is real), while transverse interactions (via the exchange of transverse plasmons) are accompanied by the collisionless Landau damping ( $\Pi_t$  is purely imaginary). Characteristic momentum transfers in transverse interactions are  $\Lambda = (\pi \omega / (4 c q_t))^{1/3} q_t \ll q_l$ , meaning that such interactions occur on larger spatial scales than the longitudinal ones. Therefore, for relativistic particles, the transverse interactions can be more efficient. The importance of such interactions was pointed out by Heiselberg and Pethick [8] in their study of kinetic properties of relativistic quark plasma. So far in all calculations of kinetic properties in neutron star cores (except for SY07) the transverse interactions have been erroneously screened by the same static dielectric function  $\Pi_l$  as the longitudinal interactions. This approximation strongly (up to several orders of magnitude) overestimates the electron-muon thermal conductivity (SY07). We will show that it overestimates also  $\eta_{e\mu}$  (but less dramatically).

The squared matrix element in (14) for free ultra-relativistic particles can be written as

$$\langle |M_{ci}|^2 \rangle = \frac{16\pi^2 \hbar^6 \alpha^2}{m_c^{*2} m_i^{*2} c^2} \varphi, \quad (18)$$

$$\frac{\langle |M_{cc}|^2 \rangle}{2} = \frac{16\pi^2 \hbar^6 \alpha^2}{m_c^{*4} c^2} (\varphi - \gamma), \quad (19)$$

where  $\varphi$  and  $\gamma$  are dimensionless functions,

$$\varphi = \varphi_{\parallel} + \varphi_{\perp} + \varphi_{\perp\parallel}, \quad (20)$$

$$\varphi_{\parallel} = \frac{(m_c^{*2} c^2 - \hbar^2 q^2/4)(m_i^{*2} c^2 - \hbar^2 q^2/4)}{\hbar^4 (q^2 + q_l^2)^2}, \quad (21)$$

$$\varphi_{\perp} = \frac{(p_{Fc}^2 - \hbar^2 q^2/4)(p_{Fi}^2 - \hbar^2 q^2/4) \cos^2 \phi + \hbar^2 (p_{Fc}^2 + p_{Fi}^2) q^2/4}{\hbar^4 (q^6 + \Lambda^6)} q^2, \quad (22)$$

$$\varphi_{\perp\parallel} = -2 \frac{\sqrt{(p_{Fc}^2 - \hbar^2 q^2/4)(p_{Fi}^2 - \hbar^2 q^2/4)}}{\hbar^4 (q^2 + q_l^2)(q^6 + \Lambda^6)} m_c^* m_i^* c^2 q^4 \cos \phi, \quad (23)$$

$\phi$  being the angle between the vectors  $\mathbf{p}_1 + \mathbf{p}_{1'}$  and  $\mathbf{p}_2 + \mathbf{p}_{2'}$ . The function  $\gamma$  describes interference between two scattering channels of identical particles. In the weak-screening approximation, its contribution is small; see Sec. II C.

## B. Effective collision frequencies

The collision frequencies are obtained by calculating the integrals (9) and (10). The calculations are greatly simplified because all particles are strongly degenerate. It is sufficient to place the colliding particles on their Fermi surfaces (whenever possible) and use the standard energy-angular decomposition based on  $d^3p = m^* p_F d\varepsilon d\Omega$ , where  $d\Omega$  is the solid angle element in the direction of  $\mathbf{p}$ . All (but one) energy integrations can be done with the aid of the energy-conserving delta-function in (14); only the  $\omega$  integration is left. Three angular integrations out of eight are performed with the aid of the momentum-conserving delta-function; three integrations (over the position of  $\mathbf{p}_1$  and over the azimuthal angle of  $\mathbf{p}_2$  with respect to  $\mathbf{p}_1$ ) are trivial and give  $8\pi^2$ . As a result, one can reduce the angular integration to the integration over  $dq$  and  $d\phi$ . Then the collision frequencies (9) and (10) can be written as

$$\nu_{ci} = \frac{12\hbar^2\alpha^2}{\pi^2 p_{Fc}^5 m_c^* c^2} (k_B T)^2 \int_0^\infty dw \frac{w^2 \exp(-w)}{[1 - \exp(-w)]^2} I_{\Omega ci}(\omega), \quad (24)$$

$$\nu'_{ci} = \frac{12\hbar^2\alpha^2}{\pi^2 p_{Fc}^5 m_i^* c^2} (k_B T)^2 \int_0^\infty dw \frac{w^2 \exp(-w)}{[1 - \exp(-w)]^2} I'_{\Omega ci}(\omega), \quad (25)$$

where  $w = \hbar\omega/(k_B T)$ . The functions  $I_{\Omega ci}(\omega)$  and  $I'_{\Omega ci}(\omega)$  are the angular integrals

$$I_{\Omega ci} = \int_0^{q_m} dq \int_0^\pi d\phi q^2 \left( p_{Fc}^2 - \frac{\hbar^2 q^2}{4} \right) \varphi, \quad (26)$$

$$I'_{\Omega ci} = - \int_0^{q_m} dq \int_0^\pi d\phi q^2 \sqrt{(p_{Fc}^2 - \hbar^2 q^2/4)(p_{Fi}^2 - \hbar^2 q^2/4)} \cos \phi \varphi, \quad (27)$$

where  $\hbar q_m = \min\{2p_c, 2p_i\}$  is the maximum momentum transfer in a collision event. Owing to a trivial integration over  $\phi$ ,  $I_{\Omega ci}$  contains two terms coming from  $\varphi_{\parallel}$  and  $\varphi_{\perp}$ , while  $I'_{\Omega ci}$  contains only the contribution from  $\varphi_{\perp}$ ,

$$I_{\Omega ci} = I_{\Omega ci}^{\parallel} + I_{\Omega ci}^{\perp}, \quad I'_{\Omega ci} = I_{\Omega ci}^{\perp}. \quad (28)$$

Let us calculate the angular integrals in the leading approximation with respect to the parameters  $\Lambda/q_m$  and  $q_l/q_m$ . This approximation is always justified for the transverse interactions because of the presence of a small quantity  $\hbar\omega \sim k_B T$  in the expression for  $\Lambda/q_m$ . However, it is less accurate for the longitudinal contribution since  $q_l/q_m$  is not too small; we will discuss corresponding corrections in Sec. II C.

The leading-order expressions for the angular integrals are

$$I_{\Omega ci}^{\perp} = \frac{\pi^2}{6\hbar^4 \Lambda} p_{Fc}^4 p_{Fi}^2, \quad (29)$$

$$I_{\Omega ci}^{\parallel} = \frac{\pi^2}{4\hbar^4} \frac{m_c^* m_i^* p_{Fc}^2 c^4}{q_l}, \quad (30)$$

$$I_{\Omega ci}^{\perp\parallel} = \frac{\pi^2 m_c^* m_i^* c^2 p_{Fc}^2 p_{Fi}^2}{2q_l \hbar^4}. \quad (31)$$

Note that the leading-order expression for  $I_{\Omega ci}^{\perp\parallel}$  is independent of  $w$ , being of the same order of magnitude with respect to  $q_l/q_m$  as  $I_{\Omega ci}^{\parallel}$ . In contrast,  $I_{\Omega ci}^{\perp} \propto w^{-1/3} \propto \Lambda^{-1}$ .

The final integration over  $w$  gives the collision frequencies

$$\nu_{ci}^{\perp} = \frac{\xi \alpha^2}{\hbar^2 c} \frac{p_{Fi}^2}{p_{Fc} m_c^* c} \left( \frac{\hbar c}{q_l^2} \right)^{1/3} (k_B T)^{5/3}, \quad (32)$$

$$\nu_{ci}^{\parallel} = \frac{\pi^2 \alpha^2 m_c^* m_i^* c^2}{\hbar^2 p_{Fc}^3 q_l} (k_B T)^2, \quad (33)$$

$$\nu'_{ci} = \frac{2\pi^2 \alpha^2 m_c^* p_{Fi}^2}{\hbar^2 p_{Fc}^3 q_l} (k_B T)^2, \quad (34)$$

where  $\xi = 2\Gamma(8/3)\zeta(5/3)(4/\pi)^{1/3} \approx 6.93$ ,  $\zeta(z)$  is the Riemann zeta function, and  $\Gamma(z)$  is the gamma function. Equations (7), (11)–(13), and (32)–(34) give  $\eta_{e\mu}$  in the weak-screening approximation.

For typical conditions in a neutron star core,

$$\nu_{ci}^{\parallel}, \nu'_{ci} \ll \nu_{ci}^{\perp}. \quad (35)$$

However, the inequality is not so strong as for the thermal conductivity (SY07). The dominance of  $\nu_{ci}^\perp$  over  $\nu_{ci}^\parallel$  is determined by the factor  $[\hbar c q_l / (k_B T)]^{1/3}$  which increases slowly with decreasing  $T$ . It is more accurate to include all components of the collision frequencies. For the thermal conductivity problem, we had  $\nu_{ci}^\perp / \nu_{ci}^\parallel \propto \hbar c q_l / (k_B T)$ , so that transverse interactions dominated at all temperatures of interest (SY07).

Nevertheless, for the not too high temperatures (see Sec. IV for details),  $\eta_{e\mu}$  is mainly determined by the collisions via the exchange of transverse plasmons. In this case, the electron and muon momentum transports are decoupled [see Eq. (11)],

$$\frac{1}{\tau_c} = \nu_c^\perp = \sum_i \nu_{ci}^\perp = \frac{\pi \xi}{4c^2} \frac{q_t}{p_{Fc} m_c^*} (\hbar c q_t)^{1/3} (k_B T)^{5/3}. \quad (36)$$

Then the shear viscosity of electrons or muons ( $c = e$  or  $\mu$ ) becomes

$$\eta_c = \eta_c^\perp = \frac{12\pi c^2 \hbar^3}{5\xi} \frac{n_c^2}{q_t (\hbar c q_t)^{1/3}} (k_B T)^{-5/3}. \quad (37)$$

We see, that in the low-temperature limit,  $\eta_{e\mu}$  has a non-standard temperature behavior,  $\eta_{e\mu} \propto T^{-5/3}$  (instead of the standard Fermi-liquid dependence  $\eta \propto T^{-2}$ ). The non-standard behavior was pointed out by Heiselberg and Pethick [8] for an ultra-relativistic quark plasma. Our results involve collisions of charged particles in the  $npe\mu$ -matter (for any degree of relativity of muons). Our expressions for  $\eta_{e\mu}$  depend only on the number densities of charged particles and on their effective masses; therefore, they can be used for any EOS of dense matter. Previous calculations [6, 13] overestimated  $\eta_{e\mu}$  because they employed the improper plasma screening of transverse interactions. Equation (37) remains valid in the presence of other charged particles (such as  $\Sigma^-$  hyperons).

### C. Corrections to the leading terms

As mentioned above, the corrections to  $\nu_c^\perp$  containing higher-order powers of  $\Lambda/q_m$  can be neglected, so that  $\nu_c^\perp$  can be taken in the form (36). In contrast, the corrections to  $\nu_c^\parallel$  containing higher-order powers of  $q_l/q_m$  can be important. At not too small temperatures, at which  $\nu_c^\parallel$  can give a noticeable contribution, such corrections can affect  $\eta_{e\mu}$ . We will discuss several corrections of this type.

#### 1. Kinematical corrections to $\nu_{ci}^\parallel$ and $\nu'_{ci}$

The main corrections to the leading terms arise from the  $q$ -dependence of the functions  $\varphi$  [Eqs. (22) and (23)] and from the  $q$ -dependence in Eqs. (26) and (27). The integral  $I_{\Omega ci}^\parallel$  is calculated precisely,

$$I_{\Omega ci}^\parallel = \frac{\pi m_c^{*2} m_i^{*2} c^4 p_{Fc}^2}{\hbar^4 q_l} I_2^\parallel(q_m/q_l) - \frac{\pi c^2 q_l}{4\hbar^2} [m_c^{*2} m_i^{*2} c^2 + p_{Fc}^2 (m_c^{*2} + m_i^{*2})] I_4^\parallel(q_m/q_l) \quad (38)$$

$$+ \frac{\pi q_l^3}{16} [(m_c^{*2} + m_i^{*2}) c^2 + p_{Fc}^2] I_6^\parallel(q_m/q_l) - \frac{\pi \hbar^2 q_l^5}{64} I_8^\parallel(q_m/q_l), \quad (39)$$

where we have introduced the integrals

$$I_k^\parallel(x) = \int_0^x \frac{x'^k}{(x'^2 + 1)^2} dx', \quad (40)$$

whose expressions are given in Appendix A. After the energy integration the corrected collision frequency becomes

$$\nu_{ci}^\parallel = \frac{4\hbar^2 \alpha^2}{p_{Fc}^5 m_c^{*2} c^2} (k_B T)^2 I_{\Omega ci}^\parallel. \quad (41)$$

Similar corrections should be calculated for  $\nu'_{ci}$ . In the leading-order approximation (with respect to  $\Lambda/q_m$ ),  $\Lambda^6$  can be neglected in the denominator of  $\varphi_{\perp\parallel}$ . The remaining angular integral is taken,

$$I_{\Omega ci}^{\perp\parallel} = \frac{\pi m_i^* m_c^{*2} c^2}{\hbar^4 q_l} \left[ p_{Fc}^2 p_{Fi}^2 I_0^{\perp\parallel}(q_m/q_l) - \frac{\hbar^2}{4} (p_{Fc}^2 + p_{Fi}^2) q_l^2 I_2^{\perp\parallel}(q_m/q_l) + \frac{\hbar^4}{16} q_l^4 I_4^{\perp\parallel}(q_m/q_l) \right], \quad (42)$$

where

$$I_k^{\perp\parallel}(x) = \int_0^x \frac{x'^k}{x'^2 + 1} dx' = I_k^{\parallel}(x) + I_{k+2}^{\parallel}(x). \quad (43)$$

After the energy integration we finally obtain

$$\nu'_{ci} = \frac{4\hbar^2\alpha^2}{p_{Fc}^5 m_i^* c^2} (k_B T)^2 I_{\Omega ci}^{\perp\parallel}. \quad (44)$$

Our calculations show that these corrections to  $\nu_{ci}^{\parallel}$  and  $\nu'_{ci}$  can reach  $\sim 70\%$ . It is advisable to include them in  $\eta_{e\mu}$ .

## 2. Corrections to lepton-proton collision frequencies

So far we have considered the function  $\varphi$  calculated for free relativistic particles. It is a good approximation for collisions within the electron-muon subsystem, because the electrons and muons constitute almost ideal Fermi gases. However, the protons belong to a strongly interacting Fermi liquid; this case should be analyzed separately. First of all we notice that the protons are non-relativistic. Moreover, we will assume, that many-body effects can be treated by introducing an effective proton mass  $m_p^*$ . Under these assumptions, the proton transition current can be written as  $J_{p2'2} \propto \frac{1}{2}(\mathbf{p}_2 + \mathbf{p}_{2'})m_p^* \delta_{\sigma_2\sigma_{2'}}$ , which only slightly modifies  $\varphi$ . The expression (23) for  $\varphi_{\perp\parallel}$  remains the same, while the two other functions become

$$\varphi_{\parallel}^{\text{cp}} = \frac{(m_c^{*2}c^2 - \hbar^2 q^2/4) m_p^{*2} c^2}{\hbar^4 (q^2 + q_l^2)^2}, \quad (45)$$

$$\varphi_{\perp}^{\text{cp}} = \frac{(p_{Fc}^2 - \hbar^2 q^2/4)(p_{Fc}^2 - \hbar^2 q^2/4) \cos^2 \phi + (p_{Fc}^2 - \hbar^2 q^2/4) \hbar^2 q^2/4}{\hbar^4 (q^6 + \Lambda^6)} q^2. \quad (46)$$

The difference between  $\nu_{cp}^{\parallel}$ , calculated with (45) and (21), is proportional to some power of  $\hbar q_l/(m_p^* c)$ . Contrary to  $q_l/q_m$ , this ratio is always small for the conditions in neutron star cores. Hence Eq. (41) with the angular integral (38) remains a valid approximation. For the completeness of our analysis, we present the modified angular integral,

$$\begin{aligned} I_{\Omega cp}^{\parallel} &= \frac{\pi m_c^{*2} m_p^{*2} c^4 p_{Fc}^2}{\hbar^4 q_l} I_2^{\parallel}(q_m/q_l) - \frac{\pi c^2 q_l m_p^{*2}}{4\hbar^2} (m_c^{*2} c^2 + p_{Fc}^2) I_4^{\parallel}(q_m/q_l) \\ &+ \frac{\pi q_l^3}{16} (m_p^{*2} c^2 + p_{Fc}^2) I_6^{\parallel}(q_m/q_l). \end{aligned} \quad (47)$$

This expression gives almost the same  $\nu_{cp}^{\parallel}$ .

## 3. Interference corrections to $\nu_{cc}$

The last correction to be discussed is the correction to  $\nu_{cc}$  (to  $\nu_{ee}$  and  $\nu_{\mu\mu}$ ) due to the interference between two scattering channels ( $1, 2 \rightarrow 1', 2'$  and  $1, 2 \rightarrow 2', 1'$ ) for collisions of identical particles. This interference is described by the dimensionless function  $\gamma$  which (like  $\varphi$ ) contains longitudinal, transverse and mixed components. An accurate consideration shows that all these components are smaller than corresponding components of  $\varphi$ . Therefore, the interference correction to  $\nu_{cc}^{\perp}$  can be neglected, and noticeable corrections can arise only to  $\nu_{cc}^{\parallel}$  and  $\nu'_{cc}$ . These corrections have been calculated in the same way as in previous sections. We have obtained that they are numerically small (give  $\lesssim 5\%$  contribution to  $\nu_{cc}^{\parallel} + \nu'_{cc}$ ). Their contribution to  $\eta_{e\mu}$  is always negligible as expected without any numerical calculations. Such corrections can be significant under two conditions. First, the longitudinal component  $\nu_{cc}^{\parallel}$  should be comparable to  $\nu_{cc}^{\perp}$ . Second,  $\nu_{cc}$  itself should give a noticeable contribution to  $\eta_{e\mu}$ . The former condition would be realized at high temperatures if particles  $c$  are weakly-relativistic. The electrons are ultra-relativistic in neutron star cores and do not obey the above requirement. The muons can be weakly-relativistic there, but if they are their contribution to  $\eta_{e\mu}$  is not large. The importance of the interference corrections in  $cc$  collisions is further reduced by a (typically) stronger contribution of  $cp$  collisions. There are also collisions between electrons and muons. The interference corrections for such collisions are absent; corresponding partial collision frequencies are of the same order of magnitude as  $\nu_{cc}$ .

Thus, the corrections to  $\nu_{cp}$  and  $\nu_{cc}$  seem to be negligible. The kinematical corrections to  $\nu_{ci}^{\parallel}$  and  $\nu_{ci}'$  are significant if  $\nu_{ci}^{\parallel}$  cannot be neglected in comparison with  $\nu_{ci}^{\perp}$ . Note that in SY07, for the electron-muon thermal conductivity problem, no corrections have been required because the thermal-conduction frequencies  $\nu_{ci}^{\perp}$  dominate at any density and temperature of practical interest.

#### 4. Comparison with exact solution

So far we have used a simplest variational solution for the shear viscosity based on the expression for the trial function (5) with  $\tau_c$  independent of the particle energy  $\varepsilon_c$ . Actually, however, the energy dependence of  $\Phi_c$  is more complicated, which affects the shear viscosity. It is convenient to introduce a correction factor  $C$  that relates the exact and variational shear viscosities,

$$\eta_{\text{exact}} = C\eta_{\text{var}}. \quad (48)$$

In ordinary Fermi-systems, where the collision probability is independent of energy transfer  $\hbar\omega$ , the factor  $C$  can be calculated using the theory developed by Sykes and Brooker [14] for one component systems and extended by Flowers and Itoh [6] and Anderson et al. [15] for multicomponent systems. Unfortunately, this theory cannot be directly applied to our case because of the dynamical character of transverse plasma screening (Landau damping).

The factor  $C$  for the thermal conductivity with account for the exchange of transverse plasmons was estimated in SY07. Let us do the same for the shear viscosity. As in SY07, we restrict ourselves to the exchange of transverse plasmons in the weak-screening approximation. Then the electron transport decouples from the muon one, and we can consider one type of momentum carriers. We redefine  $\Phi_c$  in (5) as

$$\Phi_c = -\tau_{\text{eff}} \left( v_{c\alpha} p_{c\beta} - \frac{1}{3} \delta_{\alpha\beta} v_c p_c \right) V_{\alpha\beta} \Psi(x), \quad (49)$$

where  $\tau_{\text{eff}}$  is an effective relaxation time (that can be treated as a normalization constant), and an unknown function  $\Psi(x)$  of  $x = (\varepsilon_c - \mu_c)/(k_B T)$  describes the energy dependence of  $\Phi_c$ .

Substituting (49) into the linearized kinetic equation, one obtains an integral equation for  $\Psi(x)$ ,

$$\begin{aligned} f(x)(1-f(x)) &= \frac{6\hbar^4 \alpha^2 (k_B T)^2 \tau_{\text{eff}}}{\pi^2 p_{Fc}^5 m_c^* c^2} \int_{-\infty}^{\infty} dx' \frac{x' - x}{\exp(x' - x) - 1} f(x)(1-f(x')) \\ &\times \left\{ \frac{2}{3} \frac{p_{Fc}^4}{\hbar^2} I_{\Omega c1}(x' - x)[\Psi(x) - \Psi(x')] + I_{\Omega c}(x' - x)\Psi(x') \right\}, \end{aligned} \quad (50)$$

where  $I_{\Omega c} = \sum_i I_{\Omega ci}$ ,  $I_{\Omega c1} = \sum_i I_{\Omega ci1}$ , and

$$I_{\Omega ci1} = \int_0^{q_m} dq \int_0^{\pi} d\phi \varphi. \quad (51)$$

The integral equation (50) is more complicated than that for the thermal conductivity (see Eq. (42) in SY07). The term with  $I_{\Omega c1}$  in (50) appears because we go beyond the simplest variational approach of  $\Psi_c = \text{const}$ . Without that approach, there is no cancellation of zero-order expansion terms (in series of  $q$ ) in kinematical factors in Eq. (9). It was that cancellation which led to the appearance of the  $q^2$  term under the integral in Eq. (26). The integral  $I_{\Omega ci1}$  coincides (save constant factor) with the angular integral for the thermal conductivity problem (Eq. (25) in SY07). Taking the weak-screening expressions for  $I_{\Omega c}$  and  $I_{\Omega c1}$  with the exchange of transverse plasmons alone, and choosing

$$\tau_{\text{eff}} = \left( \frac{4}{\pi} \right)^{2/3} \frac{p_{Fc} m_c^* c^2}{\alpha q_t (\hbar c q_t)^{1/3} (k_B T)^{5/3}}, \quad (52)$$

we obtain the dimensionless equation

$$\begin{aligned} \frac{1}{1 + \exp(-x)} &= \int_{-\infty}^{\infty} dx' \frac{\text{sgn}(x' - x)}{(\exp(x' - x) - 1)(1 + \exp(-x'))} \\ &\times \left[ \lambda(\Psi(x) - \Psi(x')) + |x' - x|^{2/3} \Psi(x') \right], \end{aligned} \quad (53)$$



where  $\lambda = p_{Fc}^2/(3\hbar^2\Lambda_T^2)$ . The quantity  $\Lambda_T = (\pi k_B T/(4\hbar c q_t))^{1/3} q_t$  is the transverse screening wavenumber  $\Lambda$ , with  $\hbar\omega$  replaced by  $k_B T$ . In a neutron star core, one typically has  $\hbar\Lambda_T \ll p_{Fc}$ , and hence  $\lambda \gg 1$ . If  $\lambda \sim 1$ , then the weak-screening approximation is not justified.

Once  $\Psi(x)$  is found by solving Eq. (53), the shear viscosity is given by

$$\eta_{\text{cexact}} = \frac{n_c p_{Fc}^2 \tau_{\text{eff}}}{5m_c^*} \int_{-\infty}^{\infty} dx \Psi(x) f(x) (1 - f(x)). \quad (54)$$

We have solved Eq. (53) numerically and compared the result with the variational one ( $\Psi_{\text{var}} = 2^{2/3} \pi^{2/3}/[12\xi]$ ). For  $\lambda = 10 - 1000$ , we obtain  $C = \eta_{\text{exact}}/\eta_{\text{var}} = 1.08 - 1.056$ . For  $\lambda \geq 1000$ , the factor  $C = 1.056$  becomes nearly independent of  $\lambda$ . Therefore, we have  $C \approx 1$  indicating that the simplest variational approach is well justified.

Were the electron (and muon) collisions determined solely by the exchange of longitudinal plasmons (with the transition matrix element independent of  $\omega$ ), one could find  $C$  from the standard theory. In that case one also obtains  $C \approx 1$  (see, e.g., Ref. [16]). We expect, that in the most general case, when electron and muon collisions are governed by the exchange of transverse and longitudinal plasmons, the correction factor  $C$  differs from  $C = 1$  by  $\lesssim 10\%$ . If so, the simplest variational approach is sufficiently accurate, and no corrections are required ( $C = 1$ ) for the majority of astrophysical applications.

#### D. Neutron viscosity

In this section we calculate the neutron shear viscosity  $\eta_n$ . We employ the same formalism as was used in BHY01 for studying the neutron thermal conductivity. Similar approach was used by Baiko and Haensel [16] to determine kinetic coefficients mediated by neutron-neutron collisions. We calculate  $\eta_{nn}$  from Eq. (7); the effective relaxation time of neutrons,  $\tau_n$ , is given by Eq. (11), being determined by the collision frequencies (12) of neutrons with neutrons and protons.

The neutron-neutron collision frequency can be written as

$$\nu_{nn} + \nu'_{nn} = \frac{16m_n^{*3}(k_B T)^2}{3m_n^2 \hbar^3} S_{nn} \quad (55)$$

(note that the authors of BHY01 did not separate  $\nu_{nn}$  and  $\nu'_{nn}$  but considered their sum). The neutron-proton collision frequency is

$$\nu_{np} = \frac{32m_p^{*2}m_n^*(k_B T)^2}{3m_n^2 \hbar^3} S_{np}. \quad (56)$$

Here,  $m_n$  is a bare nucleon mass. The quantities  $S_{nn}$  and  $S_{np}$  are the effective nucleon-nucleon scattering cross-sections introduced in Eq. (22) of BHY01 (for the thermal conduction problem). For the shear viscosity, in the same notations as in BHY01, we obtain

$$S_{nn} = \frac{m_n^2}{16\pi^2 \hbar^4} \int_0^1 dx' \int_0^{\sqrt{1-x'^2}} dx \frac{12x^2 x'^2}{\sqrt{1-x^2-x'^2}} \mathcal{Q}_{nn}, \quad (57)$$

$$S_{np} = \frac{m_n^2}{16\pi^2 \hbar^4} \int_{0.5-x_0}^{0.5+x_0} dx' \int_0^a dx \frac{6(x^2 - x'^2)}{\sqrt{a^2 - x^2}} \mathcal{Q}_{np}, \quad (58)$$

where  $x = \hbar q/(2p_{Fn})$ ,  $x' = \hbar q'/(2p_{Fn})$ ,  $a = \sqrt{x_0^2 - (0.25 + x_0^2 - x'^2)^2}/x'$ , and  $x_0 = p_{Fp}/(2p_{Fn})$ . This choice of integration variables is convenient for numerical integration. The quantities  $\mathcal{Q}_{nn}$  and  $\mathcal{Q}_{np}$  are squared matrix elements for nucleon-nucleon scattering (in the notations of BHY01,  $\mathcal{Q}_{nn} = \langle |M_{nn}|^2 \rangle$  and  $\mathcal{Q}_{np} = \langle |M_{np}|^2 \rangle$ ).

Let us emphasize that kinematic restrictions in Eqs. (57) and (58) are very different. The effective cross section  $S_{nn}$  is determined by a wide spectrum of momentum transfers  $q$  (or, equivalently, of scattering angles). Our calculations show that one can get a reasonably accurate  $S_{nn}$  assuming that  $\mathcal{Q}_{nn}$  is independent of  $q$ . Such a  $q$ -averaged  $\mathcal{Q}_{nn}$  can be extracted from a total neutron-neutron scattering cross section. In contrast (because, typically,  $p_{Fp} \ll p_{Fn}$ ),  $S_{np}$  is determined by small momentum transfers, that is by a small-angle cross section of neutron-proton scattering.

By analogy with BHY01, we can write  $S_{nn} = S_{nn}^{(0)} K_{nn}$  and  $S_{np} = S_{np}^{(0)} K_{np}$ . Here,  $S_{nn}$  and  $S_{np}$  are the effective cross sections calculated with in-medium squared matrix elements,  $\mathcal{Q}_{nn}$  and  $\mathcal{Q}_{np}$ ;  $S_{nn}^{(0)}$  and  $S_{np}^{(0)}$  are similar cross sections

calculated with the in-vacuum matrix elements;  $K_{nn}$  and  $K_{np}$  are the ratios of the in-medium to the in-vacuum cross sections.

The authors of BHY01 calculated all these quantities for the thermal conduction problem. The squared matrix elements  $\mathcal{Q}_{nn}$  and  $\mathcal{Q}_{np}$  were extracted from nucleon-nucleon differential scattering cross sections calculated in Refs. [17, 18] for symmetric nuclear matter with the Bonn nucleon-nucleon interaction potential using the Dirac-Brueckner approach. An accurate extraction of the in-medium  $\mathcal{Q}_{nn}$  and  $\mathcal{Q}_{np}$  required the knowledge of effective masses  $m_n^*$  and  $m_p^*$  (not reported in [17, 18]). For that reason, the procedure used in BHY01 was ambiguous. Thus, the factors  $K_{nn}$  and  $K_{np}$ , presented in BHY01 for the neutron thermal conductivity, are model dependent and not very certain.

Now we turn to calculating  $S_{nn}$ ,  $S_{np}$ ,  $S_{nn}^{(0)}$ ,  $S_{np}^{(0)}$ ,  $K_{nn}$ , and  $K_{np}$  for the shear viscosity. To avoid the above drawbacks, we suggest to neglect the in-medium effects on the squared matrix elements and set  $K_{nn} = K_{np} = 1$ ,  $S_{nn} = S_{nn}^{(0)}$ , and  $S_{np} = S_{np}^{(0)}$ . According to BHY01 (for the thermal conductivity),  $K_{nn}$  and  $K_{np}$  are indeed  $\sim 1$  (and  $K_{np}$  is relatively unimportant). Recently Zhang et al. [12] have studied nucleon-nucleon scattering cross sections in nuclear matter taking into account two-nucleon and three-nucleon interactions. They used the Brueckner-Hartree-Fock approach and the Argonne V14 nucleon-nucleon interaction model supplemented by three-nucleon interactions. Their principal conclusion is that the in-medium effects on square matrix elements are relatively weak, while the main medium effect consists in modifying (mostly reducing)  $m_n^*$  and  $m_p^*$ . The reduction of effective masses under the simultaneous effects of two-nucleon and three-nucleon forces is much stronger than under the effect of two-nucleon forces alone.

Thus, we have calculated  $\mathcal{S}_{nn}$  and  $\mathcal{S}_{np}$  from Eqs. (57) and (58) using the in-vacuum matrix elements  $\mathcal{Q}_{nn}$  and  $\mathcal{Q}_{np}$  from Refs. [17, 18]. These matrix elements accurately reproduce [19] well elaborated laboratory measurements of differential nucleon-nucleon scattering cross sections. Our calculations of  $\mathcal{S}_{nn}$  and  $\mathcal{S}_{np}$  are expected to be very close to those done with in-vacuum cross sections measured in laboratory. In this sense, our values of  $\mathcal{S}_{nn}$  and  $\mathcal{S}_{np}$  are model independent. Similar calculations of  $\mathcal{S}_{nn}$  in Ref. [16] give slightly different results due to the different data sets for  $\mathcal{Q}_{nn}$ . Because our equations (55) and (56) for the nucleon-nucleon collision frequencies contain a proper dependence on  $m_n^*$  and  $m_p^*$ , they can be regarded as *independent* of any specific model for nucleon-nucleon interaction. It can be a two-body or two-body plus three-body interaction; its explicit form is not essential. Thus, we obtain a description of the neutron shear viscosity valid for any EOS of nucleon matter. This approach is not strict (uses the in-vacuum matrix elements) but universal. One can in principle calculate more accurate in-medium matrix elements for any chosen EOS but loosing the universality. For calculating the diffusive thermal conductivity from the equations of BHY01, we would recommend to adopt the same approach and set  $K_{nn} = K_{np} = 1$  in those equations.

The results of our calculations can be fitted by the expressions

$$\begin{aligned} S_{nn} &= \frac{12.88}{k_n^{1.915}} \frac{1 - 0.6253k_n + 0.3305k_n^2}{1 - 0.0736k_n} \text{ mb}, \\ S_{np} &= \frac{0.8876 k_p^{3.5}}{k_n^5} \frac{1 + 139.6k_p + 103.7k_n}{1 - 0.5932k_n + 0.1829k_n^2 + 7.629k_p^2 - 0.5405k_p k_n} \text{ mb}, \end{aligned} \quad (59)$$

where  $k_i$  is the Fermi wavenumber of nucleons  $i$  expressed in  $\text{fm}^{-1}$ . As in BHY01, the calculations and fits cover the range of  $k_n$  from 1.1 to 2.6  $\text{fm}^{-1}$  and the range of  $k_p$  from 0.3 to 1.2  $\text{fm}^{-1}$ . These parameter ranges are appropriate to neutron star cores at  $0.5\rho_0 \lesssim \rho \lesssim 3\rho_0$ . The fit errors for  $S_{nn}$  do not exceed 0.5%. The maximum fit error of  $S_{np}$  is  $\delta_{\max} \sim 8\%$  (at  $k_n = 1.1 \text{ fm}^{-1}$  and  $k_p = 0.7 \text{ fm}^{-1}$ ).

### III. SHEAR VISCOSITY IN SUPERFLUID MATTER

Neutrons and protons in the npe $\mu$ -matter of neutron star cores can be in superfluid state (e.g., Ref. [5]). Here, we study the effects of superfluidity on the shear viscosity. Let  $T_{cn}(\rho)$  be the critical temperature for superfluidity of neutrons, and  $T_{cp}(\rho)$  be the same for protons. Proton superfluidity means superconductivity. Calculations of superfluid critical temperatures are complicated and very sensitive to a chosen model of nucleon-nucleon interaction and a method to employ many-body (polarization) effects [5]. Numerous calculations give drastically different  $T_{cn}(\rho)$  and  $T_{cp}(\rho)$ . It is instructive not to rely on any particular model but treat  $T_{cn}$  and  $T_{cp}$  as free parameters varied within reasonable limits ( $T_c \lesssim 10^{10} \text{ K}$ ), in accordance with microscopic calculations.

Neutron superfluidity has no direct effect on the shear viscosity  $\eta_{e\mu}$  of electrons and muons (because  $\eta_{e\mu}$  is limited by electromagnetic interactions). However, it strongly affects neutron star hydrodynamics in a complicated way. It makes the hydrodynamics essentially multifluid (with several hydrodynamical velocity fields; e.g., [20] and references therein); it introduces an entrainment effect (which relates motion of neutrons and protons), creates a very specific spectrum of elementary medium excitations (phonons) and associated specific energy and momentum transfer mechanisms. All these problems go far beyond the scope of our paper. Therefore, we will neglect the effects of neutron superfluidity

(will treat neutrons as normal) but consider the effects of proton superfluidity on  $\eta_n$  (assuming the protons to be passive scatterers of neutrons, i.e., ignoring momentum transport by protons). We disregard thus hydrodynamical effects of neutron and proton superfluids.

Microscopically, proton superfluidity manifests itself in rearranging proton states (from normal Fermi-liquid quasiparticles to Bogoliubov quasiparticles) and in the appearance of a gap  $\Delta$  in the proton energy spectrum near the Fermi level ( $\varepsilon = \mu$ ),

$$\varepsilon = \mu + \text{sgn}(\xi)\sqrt{\Delta^2 + \xi^2}, \quad (60)$$

where  $\xi \equiv v_F(p - p_F)$ ; the presented equation is valid at  $|\xi| \ll \mu$ .

It is generally believed, that Cooper paring of protons appears in the singlet  $^1S_0$  state (e.g., Ref. [5]). The temperature dependence of  $\Delta$ , calculated in the BCS approximation, can be approximated as [21]

$$y = \frac{\Delta}{k_B T} = \sqrt{1 - \tau} \left( 1.456 - \frac{0.157}{\sqrt{\tau}} + \frac{1.764}{\tau} \right), \quad (61)$$

where  $\tau = T/T_{cp}$ .

### A. The effects of proton superfluidity on the electron-muon viscosity

The effects of proton superfluidity on  $\eta_{e\mu}$  are twofold. First, proton superfluidity affects the plasma dielectric function and, hence, the screening of electromagnetic interactions. The longitudinal dielectric function is almost insensitive to the presence of superfluidity [22], while the transverse dielectric function modifies and changes collision frequencies  $\nu_{ci}^\perp$ . The frequencies  $\nu_{ci}'$  remain almost unchanged because they are independent of the transverse screening in the leading order.

As in SY07, a collision frequency in superfluid matter (to be denoted as  $\nu_{ci}^{\perp S}$ ) can be written as

$$\nu_{ci}^{\perp S} = \nu_{ci}^\perp R_l^\perp(y, r), \quad (62)$$

where  $\nu_{ci}^\perp$  ( $i = e, \mu$ ) stands for a collision frequency in non-superfluid matter, while  $R_l^\perp(y, r)$  accounts for the superfluid effects (which mainly reduce the collision rate);

$$r = (p_{Fe}^2 + p_{F\mu}^2)/p_{Fp}^2 \quad (63)$$

is a slowly varying function determined by plasma composition. We have  $r = 1$  in the absence of muons, and  $r > 1$  in the presence of muons, with the maximum value of  $r \approx 1.26$  in the limit of ultra-relativistic muons. The reduction factor  $R_l^\perp(y, r)$  for the shear viscosity is, however, not the same as for the thermal conductivity (obtained in SY07) and will be calculated below.

The second effect of proton superfluidity consists in an additional (direct; not through plasma screening) reduction of the lepton-proton collision frequencies (such as  $\nu_{ep}$  and  $\nu_{\mu p}$ ). This direct reduction is exponential; it can be described by the reduction factors

$$\nu_{cp}^{\perp S} = \nu_{cp}^\perp R_p^\perp(y, r), \quad (64)$$

$$\nu_{cp}^{\parallel S} = \nu_{cp}^\parallel R_p^\parallel(y). \quad (65)$$

The reduction factors  $R_p^\perp$  and  $R_p^\parallel$  are not the same due to the difference in longitudinal and transverse plasma screenings. Following SY07, it is convenient to introduce the reduction factor  $R_{tot}^\perp$  for the total transverse collision frequency  $\nu_c^\perp = \nu_{ce}^\perp + \nu_{c\mu}^\perp + \nu_{cp}^\perp$ ,

$$\nu_c^{\perp S} = \nu_c^{\perp S} R_{tot}^\perp(y, r), \quad (66)$$

$$R_{tot}^\perp(y, r) = [r R_l^\perp(y, r) + R_p^\perp(y, r)] / (r + 1). \quad (67)$$

Below we calculate  $R_l^\perp$ ,  $R_p^\perp$ ,  $R_p^\parallel$ , and  $R_{tot}^\perp$ .

### 1. Superfluid reduction of collisions in electron-muon subsystem

Superfluid reduction of lepton-lepton collisions is governed by the transverse polarization function  $\Pi_t$ . For the conditions in neutron star cores, it is sufficient to use  $\Pi_t$  in the so-called Pippard limit ( $\hbar\omega \ll p_{Fp}v_{Fp}$ ,  $\hbar q \ll p_{Fp}$  and  $\xi \gg 1/q$ , where  $\xi \sim \hbar v_{Fp}/(k_B T_{cp})$  is the coherence length). In this approximation, the proton contribution to  $\Pi_t$  reads

$$\Pi_t^{(p)} = \frac{q_{tp}^2}{4} \frac{\Delta}{\hbar c q} Q(w, y), \quad (68)$$

where  $q_{ti}^2 = 4\alpha p_{Fi}^2/(\hbar^2\pi)$ , and  $Q$  is the response function calculated in Ref. [23] and discussed in SY07 in more details.

In the non-superfluid limit of  $y \ll 1$  one has  $Q = i\pi\hbar\omega/y$ , which corresponds to the standard Landau-damping expression. In the opposite case of strong superfluidity ( $y \gg 1$ ), the response function  $Q$  becomes pure real,  $Q = \pi^2$ . For intermediate superfluidity,  $y \sim 1$ , we have used the expressions for  $Q$  derived in [23]. They are valid for a pure BCS formalism neglecting collective modes and related vortex renormalization in current operators due to gradient invariance. However, as in SY07, the main contribution to  $\eta_{e\mu}$  comes from the parameter values far from characteristic frequencies of collective modes (far from  $\omega \sim v_F q$ ) and we can use the standard BCS theory.

The expression for the total polarization function in the superfluid case takes the form

$$\Pi_t = \frac{\pi\omega}{4qc} \left\{ q_{tp}^2 \frac{y}{\pi w} \Re Q(w, y) + i \left[ q_{te}^2 + q_{t\mu}^2 + q_{tp}^2 \frac{y}{\pi w} \Im Q(w, y) \right] \right\}. \quad (69)$$

In the case of strong superfluidity, the main contribution to  $\Pi_t$  comes from protons. Moreover, the character of plasma screening changes. Instead of the dynamical Landau damping, the screening becomes static, with the frequency-independent screening wave number  $\Lambda_S = [\pi^2 q_{tp}^2 \Delta / (4\hbar c)]^{1/3}$ . In neutron star cores, one typically has  $\Delta \sim k_B T_{cp} \ll p_{Fi}c$ . Therefore, the relation  $\Lambda_S \ll q_l$  remains true in the superfluid case. In other words, the exchange of transverse plasmons in proton superfluid remains more efficient than the exchange of longitudinal plasmons. The strong inequality  $\Lambda_S \ll q_m$  justifies the use of the leading-order weak screening approximation in describing the exchange of transverse plasmons.

In order to calculate the reduction factor  $R_l^\perp$  one should reconsider the transverse angular integral  $I_{\Omega ci}^\perp$  taking into account the changes of electrodynamical plasma properties in superfluid matter. In the leading order with respect to  $\Lambda_S/q_m$ ,

$$I_{\Omega ci}^{\perp S} = I_{\Omega ci}^\perp F^\perp(w, y, r), \quad (70)$$

where  $I_{\Omega ci}^\perp$  refers to non-superfluid matter, while

$$\begin{aligned} F^\perp(w, y, r) &= \frac{[\pi w(r+1)]^{1/3} \left[ (\pi w r + y \Im Q(w, y))^2 + (y \Re Q(w, y))^2 \right]^{1/3}}{|\pi w r + \Delta \Im Q(w, y)|} \\ &\times \frac{2}{\sqrt{3}} \sin \left[ \frac{2}{3} \arctan \frac{|\pi w r + y \Im Q(w, y)|}{y \Re Q(w, y)} \right] \end{aligned} \quad (71)$$

accounts for superfluid effects. In the limit of strong superfluidity ( $y \gg 1$ ) we have

$$F^\perp(w, y, r) = \frac{4}{3\sqrt{3}} \left[ \frac{w(r+1)}{\pi y} \right]^{1/3}. \quad (72)$$

This asymptotic  $w$ -dependence compensates the  $w$ -dependence in  $I_{\Omega ci}^{\perp S}$  (that appeared under the effect of plasma screening). Moreover, in the expression for  $I_{\Omega ci}^{\perp S}$  the collision energy  $\hbar\omega$  is now replaced by the energy gap  $\Delta$ .

Finally, we write  $\nu_{ci}^{\perp S} = \nu_{ci}^\perp R_l^\perp(y, r)$ , and the reduction factor becomes

$$R_l^\perp(y, r) = \frac{1}{\Gamma(8/3)\zeta(5/3)} \int_0^\infty \frac{\exp(w)}{[\exp(w) - 1]^2} w^{5/3} F^\perp(w, y, r) dw. \quad (73)$$

When superfluidity vanishes ( $y \rightarrow 1$ ) we evidently have  $R_l^\perp(y, r) \rightarrow 1$ . In the opposite case of strong superfluidity ( $y \gg 1$ ) we obtain

$$R_l^\perp(y, r) = \frac{4\pi^2}{9\sqrt{3}\Gamma(8/3)\zeta(5/3)} \left( \frac{r+1}{\pi y} \right)^{1/3}. \quad (74)$$

Thus, strong proton superfluidity restores the temperature dependence  $\nu_{ci}^{\perp S} \propto T^2$  that is standard for Fermi systems. This result was derived in SY07 for the thermal conduction problem. It is a natural consequence of changing plasma screening from dynamical to statical one when  $T$  falls below  $T_{cp}$ .

In addition, we have computed  $R_l^{\perp}(y, r)$  for a wide grid of  $y$ . We do not present an appropriate fit, because we will calculate and fit the total reduction factor  $R_{tot}^{\perp}(y, r)$  for  $\nu_c^{\perp}$ .

## 2. Superfluid reduction of collisions of electrons and muons with protons

Now consider a direct effect of superfluidity on electron-proton and muon-proton collision rates. The consideration is similar to that for the thermal conduction problem (SY07). The proton energy gap has to be included in the expressions for the collision frequencies through the proton Fermi-Dirac distributions. In addition, the electron-proton and muon-proton scattering matrix elements have to be calculated using wave functions of proton Bogoliubov quasiparticles. As a result, the reduction factors  $R_p^{\perp}(y)$  and  $R_p^{\parallel}(y, r)$  can be written as

$$R_p^{\perp}(y, r) = \frac{1}{\Gamma(8/3)\zeta(5/3)} \int_0^{\infty} \int_0^{\infty} \frac{dx_2 dx_{2'}}{1 + \exp(z_2)} \times \left\{ \frac{(z_{2'} - z_2)|z_{2'} - z_2|^{-1/3} (1 + 4u_2 u_{2'} v_2 v_{2'})}{[1 + \exp(-z_{2'})][\exp(z_{2'} - z_2) - 1]} F^{\perp}(|z_{2'} - z_2|, y, r) \right. \quad (75)$$

$$\left. - \frac{(z_{2'} + z_2)|z_{2'} + z_2|^{-1/3} (1 - 4u_2 u_{2'} v_2 v_{2'})}{[1 + \exp(z_{2'})][\exp(-z_{2'} - z_2) - 1]} F^{\perp}(|z_{2'} + z_2|, y, r) \right\}, \quad (76)$$

$$R_p^{\parallel}(y) = \frac{3}{\pi^2} \int_0^{\infty} \int_0^{\infty} \frac{dx_2 dx_{2'}}{1 + \exp(z_2)} \left\{ \frac{(z_{2'} - z_2)(1 - 4u_2 u_{2'} v_2 v_{2'})}{[1 + \exp(-z_{2'})][\exp(z_{2'} - z_2) - 1]} \right. \quad (77)$$

$$\left. - \frac{(z_{2'} + z_2)(1 + 4u_2 u_{2'} v_2 v_{2'})}{[1 + \exp(z_{2'})][\exp(-z_{2'} - z_2) - 1]} \right\}, \quad (78)$$

where

$$u_p = \frac{1}{\sqrt{2}} \sqrt{1 + \frac{x}{z}}, \quad v_p = \frac{\text{sgn}(x)}{\sqrt{2}} \sqrt{1 - \frac{x}{z}}, \quad (79)$$

$x = v_{Fp}(p - p_{Fp})/(k_B T)$  and  $z = (\varepsilon - \mu_p)/(k_B T)$ .

In the limit of strong superfluidity ( $y \gg 1$ ) we obtain  $R_p^{\parallel}(y) = A^{\parallel} \exp(-y)$  and  $R_p^{\perp}(y, r) = A^{\perp}(r+1)^{1/3} y^{2/3} \exp(-y)$ , where

$$A^{\parallel} = \frac{6}{\pi^2} \int_0^{\infty} d\eta_1 \int_0^{\infty} d\eta_2 \frac{(\eta_1^2 - \eta_2^2)(\eta_1^2 + \eta_2^2)}{\exp(\eta_1^2) - \exp(\eta_2^2)} \approx 1.45425 \quad (80)$$

and

$$A^{\perp} = \frac{16}{3\sqrt{3}\pi^{1/3}\Gamma(8/3)\zeta(5/3)} \int_0^{\infty} d\eta_1 \int_0^{\infty} d\eta_2 \frac{\eta_1^2 - \eta_2^2}{\exp(\eta_1^2) - \exp(\eta_2^2)} \approx 0.92974. \quad (81)$$

Thus, at  $T \ll T_{cp}$  collisions with superfluid protons are exponentially suppressed. Then the shear viscosity  $\eta_{e\mu}$  is limited by collisions within the electron-muon subsystem (which are also affected by proton superfluidity as described in Sec. III A 1).

We have computed  $R_p^{\parallel}(y)$  for a wide range of  $y$  and fitted the results by the expression

$$R_p^{\parallel}(y) = \left\{ A^{\parallel} + (1.25 - A^{\parallel}) \exp(-0.0437 y) + (1.473 y^2 + 0.00618 y^4) \exp \left[ 0.42 - \sqrt{(0.42)^2 + y^2} \right] \right\} \times \exp \left[ -\sqrt{(0.22)^2 + y^2} \right], \quad (82)$$

which reproduces also the asymptotic limits. The maximum relative fit error is 0.75% at  $y = 0.533$ .

We do not present a separate fit expression for  $R_p^\perp(y, r)$ , but give the fit of the total reduction factor  $R_{tot}^\perp(y, r)$ :

$$\begin{aligned} R_{tot}^\perp &= \frac{1 - g_1}{(1 + g_3 y^3)^{1/9}} + (g_1 + g_2) \exp \left[ 0.145 - \sqrt{(0.145)^2 + y^2} \right], \\ g_1 &= 0.87 - 0.314r, \quad g_2 = (0.423 + 0.003r)y^{1/3} + 0.0146y^2 - 0.598y^{1/3} \exp(-y), \\ g_3 &= 251r^{-9}(r+1)^6(1-g_1)^9, \end{aligned} \quad (83)$$

with the maximum fit error  $\sim 0.3\%$  at  $r = 1$  and  $y = 3.5$ . This fit reproduces also the limiting case of  $R_{tot}^\perp \rightarrow 1$  at  $y \rightarrow 0$ , and the asymptote at  $y \gg 1$ ,

$$R_{tot}^\perp(y, r) = \frac{4\pi^2 r}{9\sqrt{3}\Gamma(8/3)\zeta(5/3)(r+1)^{2/3}} \frac{1}{(\pi y)^{1/3}}. \quad (84)$$

Recently the electron shear viscosity in superfluid matter has been analyzed by Andersson et al. [7]. These authors have used the standard (but approximate) approach in which the transverse plasma screening is assumed to be the same as the longitudinal one. This approach is inaccurate even in the non-superfluid case. In Ref. [7] the effects of superfluidity are described by a reduction factor  $R_{ep}^*$  for the effective electron-proton collision frequency. That factor has been taken from Ref. [24] devoted to the thermal conductivity problem. However, the reduction factors for the thermal conductivity and shear viscosity are different. Moreover, the factor  $R_{ep}^*$  in [7] is inaccurate even for the thermal conductivity, because it assumes approximate plasma screening and neglects additional terms associated with creation/annihilation of proton Bogoliubov quasiparticles; see SY07 for details. Nevertheless, numerical values of  $\eta_e$ , derived from the results of [7] for superfluid matter, are not too different from our results. Typically, they overestimate  $\eta_e$  by a factor of three, and this overestimation increases with decreasing  $T_{cp}$ .

In the limit of strong superfluidity, the temperature dependence of  $\nu_c^{\perp S}$  formally restores the standard Fermi-liquid behavior,  $\nu_c^{\perp S} \propto T^2$ . Therefore,  $\nu_{ci}^\parallel$  can be comparable to  $\nu_c^{\perp S}$ . Note, that the ratio  $\nu_{ci}^\parallel/\nu_c^{\perp S}$  in superfluid matter remains approximately the same as its value at  $T = T_{cp}$ . If  $T_{cp}$  is sufficiently small, then at  $T = T_{cp}$  we have  $\nu_c^\perp \gg \nu_{ci}^\parallel$ , and the same inequality holds at smaller  $T$ . The shear viscosity in superfluid matter, fully determined by the exchange of transverse plasmons, can be written as

$$\eta_c^{\perp S} = \frac{\xi_S}{(k_B T)^2} \frac{n_c^2}{\alpha^{2/3}} \frac{\hbar^4 c^2 p_{Fp}}{p_{Fe}^2 + p_{F\mu}^2} \left( \frac{\Delta}{p_{Fp} c} \right)^{1/3}, \quad \xi_S = \frac{27\sqrt{3}\pi^{1/3}}{40} \approx 1.71. \quad (85)$$

One can use this expression for estimates, but we recommend to employ the total collision frequency in practical calculations.

## B. Neutron shear viscosity in superfluid matter

We study the effect of proton superfluidity on neutron-proton collisions. Even this problem is difficult and we adopt a simplified approach used in BHY01 for the problem of neutron thermal conductivity. It has also been widely used for analyzing superfluid suppression of various neutrino processes (e.g., [25] and references therein). It consists in taking an ordinary differential probability of a given scattering process (neutron-proton scattering, in our case) and inserting particle energies (60) with energy gaps in corresponding Fermi-Dirac distribution functions. In our case, this approach is expected to be sufficiently accurate. Let us recall that we consider the protons only as neutron scatterers. Proton superfluidity suppresses this scattering channel, and our approach reproduces such a suppression.

In this approximation, the neutron-proton collision frequency becomes

$$\nu_{np}^S = \nu_{np} R_{np}(y), \quad (86)$$

where  $R_{np}(y)$  is the superfluid reduction factor. The latter factor is given by the same expression as the reduction factor for lepton-proton collisions,  $R_p^\parallel$ , save the coherence factors,

$$\begin{aligned} R_{np}(y) &= \frac{3}{\pi^2} \int_0^\infty \int_0^\infty \frac{dx_2 dx_{2'}}{1 + \exp(z_2)} \left\{ \frac{z_{2'} - z_2}{[1 + \exp(-z_{2'})][\exp(z_{2'} - z_2) - 1]} \right. \\ &\quad \left. - \frac{z_{2'} + z_2}{[1 + \exp(z_{2'})][\exp(-z_{2'} - z_2) - 1]} \right\}. \end{aligned} \quad (87)$$

It obeys the asymptotes  $R_{\text{np}}(0) = 1$  and  $R_{\text{np}}(y) \rightarrow A_{\text{np}} y \exp(-y)$  at  $y \rightarrow \infty$ , where  $A_{\text{np}} = 0.8589$ .

We have calculated  $R_{\text{np}}(y)$  in a wide range of  $y$  and fitted the results by the expression

$$R_{\text{np}}(y) = \frac{2}{3} \left[ 0.513 + \sqrt{(0.487)^2 + 0.018 y^2} \right] \exp \left[ 2.26 - \sqrt{(2.26)^2 + y^2} \right] + \frac{1}{3} (1 + 0.00056 y^4) \exp \left[ 6.2 - \sqrt{(6.2)^2 + 4 y^2} \right]; \quad (88)$$

the formal maximum fit error is  $\approx 0.25\%$  at  $y = 11.6$ .

Note, that proton superfluidity affects  $\eta_{\text{n}}$  weaker than  $\eta_{\text{e}\mu}$  (because of a relatively small contribution of neutron-proton collisions to  $\eta_{\text{n}}$ ).

## IV. RESULTS AND DISCUSSION

### A. Equations of state

Our results can be used for a wide range of EOSs of the npe $\mu$ -matter in neutron star cores. For illustration, we have selected five model EOSs. The parameters of these EOSs are given in Table I, including the maximum gravitational mass  $M_{\text{max}}$  of stable stars and the threshold density  $\rho_{\mu}$  of muon appearance.

Table I: Parameters of the selected EOSs: The compression modulus  $K_0$  of symmetric saturated nuclear matter; the muon threshold density  $\rho_{\mu}$ ; and also the central density  $\rho_{\text{max}}$ , the mass  $M_{\text{max}}$  and radius  $R_{\text{m}}$  of maximum-mass models ( $\rho_{\mu}$  and  $\rho_{\text{max}}$  are given in units of  $10^{14} \text{ g cm}^{-3}$ )

EOS	$K_0$ MeV	$\rho_{\mu 14}$	$\rho_{\text{max} 14}$	$M_{\text{max}}$ $M_{\odot}$	$R_{\text{m}}$ km
APR	237	2.28	27.6	1.923	10.31
	120	2.55	38.6	1.468	9.18
PAL I	180	2.55	31.4	1.738	9.92
	240	2.55	26.6	1.950	10.59
	120	2.58	35.3	1.484	9.72
PAL II	180	2.58	29.5	1.753	10.36
	240	2.58	25.3	1.966	10.97
	120	2.46	44.4	1.416	8.45
PAL III	180	2.46	34.5	1.713	9.60
	240	2.46	28.6	1.910	10.12
	120	2.50	42.0	1.438	8.75
PAL IV	180	2.50	33.2	1.713	9.60
	240	2.50	27.8	1.927	10.32

The APR EOS was constructed by Akmal, Pandharipande, and Ravenhall [26] (their model Argonne V18+ $\delta v$ +UIX\*); it is often used in the literature. Specifically, we adopt its convenient parametrization proposed by Heiselberg and Hjorth-Jensen [27] and described as APR I by Gusakov et al. [28]. It is sufficiently stiff, the maximum neutron star mass is  $M_{\text{max}} \approx 1.92 M_{\odot}$  (and the maximum-mass star has circumferential radius of  $R_{\text{m}} = 10.31 \text{ km}$ ), the muons appear at  $\rho_{\mu} \approx 2.28 \times 10^{14} \text{ g cm}^{-3}$ ; see Table I.

The PAL EOSs are convenient semi-analytical phenomenological EOSs proposed by Prakash, Ainsworth, and Latimer [29]. They differ by the functional form of the dependence of the symmetry energy  $S$  of dense matter on the baryon number density  $n_b$ . This dependence is described [29] by a function  $F(u)$ , where  $u = n_b/n_0$ ,  $n_0 = 0.16 \text{ fm}^{-3}$  being the baryon number density of saturated symmetric matter. For the PAL EOSs I, II, and III, these functions are  $F(u) = u$ ,  $2u^2/(u+1)$ , and  $\sqrt{u}$ , respectively. The PAL IV EOS belongs to the same family of EOSs, but with the symmetry energy  $S(u) \propto u^{0.7}$  suggested by Page and Applegate [30]. The PAL EOSs differ also [29] by the value of the compression modulus  $K_0$  of saturated symmetric matter,  $K_0 = 120, 180$ , and  $240 \text{ MeV}$ . Nevertheless, the particle fractions  $n_i/n_b$  as a function of  $n_b$  are independent of  $K_0$  (for these EOSs); the dependence of  $n_b$  on  $\rho$  is almost identical for the three selected  $K_0$  values [at a fixed  $F(u)$ ]. Hence, the collision frequencies and the shear viscosity are

independent of  $K_0$ . However, taking different  $K_0$ , one obtains very different neutron star models (different mass-radius relations and  $M_{\text{max}}$ ; see Table I). For illustration, we take  $K_0 = 240$  MeV for all PAL models (unless the contrary is indicated).

Therefore, our selected EOSs correspond to a large variety of neutron star models.

### B. Shear viscosity in non-superfluid matter

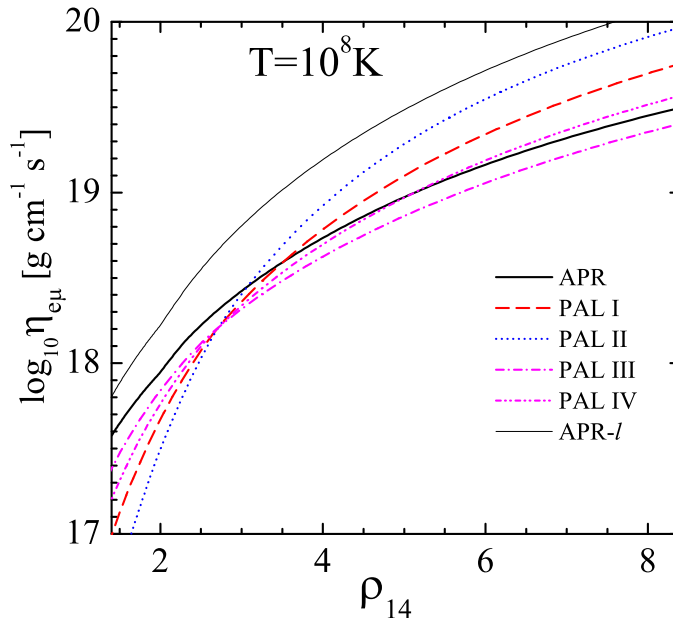


Figure 1: (Color online) Shear viscosity  $\eta_{e\mu}$  of electrons and muons versus density  $\rho_{14}$  (in units of  $10^{14}$  g cm $^{-3}$ ) for different EOSs (Table I) at  $T = 10^8$  K ( $m_p^* = 0.8 m_n$ ). The thin solid line (APR- $l$ ) shows the viscosity  $\eta_{e\mu}$  calculated with account for the exchange of longitudinal plasmons alone.

Figure 1 shows the shear viscosity  $\eta_{e\mu}$  of electrons and muons versus density at  $T = 10^8$  K for five EOSs. The given temperature is typical for middle-aged ( $t \sim 10^4 - 10^5$  yr) isolated (cooling) neutron stars without enhanced neutrino emission in their cores (e.g., Refs. [25, 30]). The proton effective mass is taken to be  $m_p^* = 0.8 m_n$ . The thick lines give  $\eta_{e\mu}$  for the APR and PAL I–IV EOSs, while the thin solid line is for the APR EOS, but it is calculated including the contribution from the exchange of longitudinal plasmons alone. One can see, that the inclusion of transverse plasmons lowers  $\eta_{e\mu}$  by a factor of three at  $\rho \gtrsim 4 \times 10^{14}$  g cm $^{-3}$ . With the fall of temperature this lowering is stronger. The exchange of transverse plasmons has not been included in previous calculations of the shear viscosity in neutron star cores, which has resulted in an overestimation of  $\eta_{e\mu}$ . The viscosity  $\eta_{e\mu}$  for the PAL II EOS (the dotted line) goes significantly higher than other curves due to a larger amount of protons (and, therefore, electrons and muons) for this EOS.

Figure 2 demonstrates the density dependence of the neutron shear viscosity multiplied by squared temperature,  $\eta_n T^2$ . This combination is temperature independent. The curves are calculated assuming the nucleon effective masses  $m_n^* = m_p^* = 0.8 m_n$ . In principle, the effective masses can be taken from microscopic calculations of an EOS; they can depend on  $\rho$ , and our expressions for the shear viscosity allow one to incorporate this density dependence. Here we assume density independent effective masses by way of illustration. In Fig. 2, for simplicity, we do not present the results for the PAL IV EOS; they are very close to the APR results. One can see, that the neutron viscosity for the selected EOSs differs within a factor of  $\lesssim 2$ .

Figure 3 demonstrates the viscosity approximation of Cutler and Lindblom [2] (curve CL) versus  $\rho$  at  $T = 10^7$  K. Recall that the approximation is based on the calculations by Flowers and Itoh [6] performed for the EOS of Baym, Bethe and Pethick [31] assuming in-vacuum nucleon-nucleon scattering cross sections and  $m_n^* = m_p^* = m_n$ . Also, we show self-consistent calculations of  $\eta_n$  by Benhar and Valli [10] for a pure neutron matter with the EOS that is basically similar to APR (with another version for three-nucleon interaction). The authors have used one and the same nucleon interaction potential to derive the EOS and  $\eta_n$ . The curve BV (2bf) is their result (from their Fig. 1)



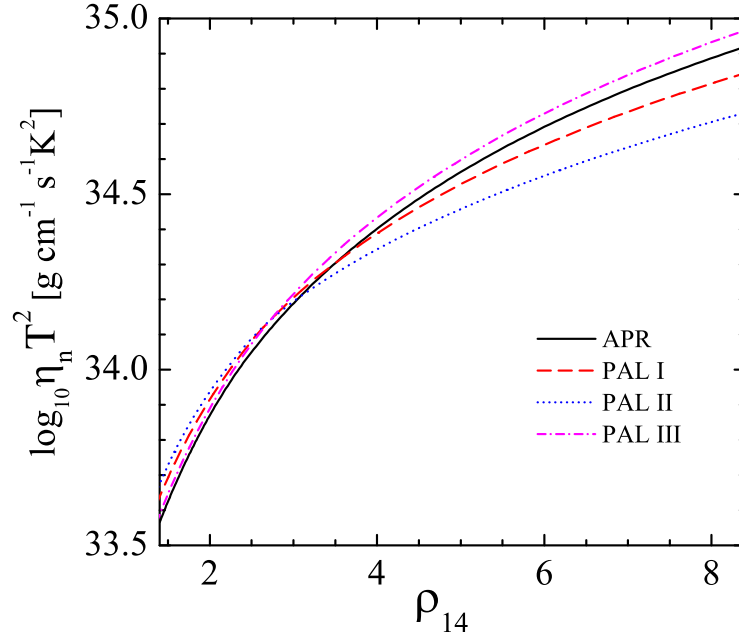


Figure 2: (Color online) Viscosity  $\eta_n$  of neutrons times  $T^2$  versus density for four EOSs ( $m_n^* = m_p^* = 0.8 m_n$ ).

obtained employing two-body nucleon forces; the curve BV (2bf+3bf) is obtained employing the two-body and three-body forces. The effective mass  $m_n^*$  is calculated self-consistently as a function of  $\rho$  ( $m_n^*$  is different for both curves and, unfortunately, is not reported in [10]).

All other curves in Fig. 3 are our results for the APR EOS assuming various values of  $m_n^*$  and  $m_p^*$ . For simplicity, these phenomenological values are taken density independent. We show either the viscosity  $\eta_{nn}$ , limited by neutron-neutron collisions alone (dashed lines), or the viscosity  $\eta_n$ , limited by neutron-neutron and neutron-proton collisions (solid lines). One can see that the contribution of neutron-proton collisions is relatively small, while the dependence of the viscosity on nucleon effective masses is important. Smaller effective masses strongly increase the neutron viscosity. In the limit of  $m_n^* = m_p^* = m_n$  we obtain the viscosity  $\eta_n$  which is a factor of  $\approx 40$  smaller than CL. Using the results of BHY01 for the thermal conductivity of neutrons  $\kappa_n$ , derived in the same approximations as our results for  $\eta_n$ , we obtain the values of  $\kappa_n$  a factor of 2–4 smaller than those given by Flowers and Itoh [6, 32]. The nature of this systematic disagreement of our results with the results of Flowers and Itoh is unclear. We have checked that it cannot be attributed to using different EOSs.

A comparison of our results with those of Benhar and Valli [10] is complicated because Benhar and Valli do not present the values of  $m_n^*$  which they obtained for a neutron matter. If, however, we take a reasonable value of  $m_n^* = 0.7 m_n$ , we obtain  $\eta_{nn}$  (not shown in Fig. 3) very close to the curve BV (2bf) of Benhar and Valli. In order to reproduce their BV (2bf+3bf) curve with our equations, we should employ a density dependent  $m_n^*$ . It should vary from  $m_n^* \approx 0.6 m_n$  at  $\rho \sim 1.5 \times 10^{14} \text{ g cm}^{-3}$  to  $0.45 m_n$  at  $\rho \sim 6 \times 10^{14} \text{ g cm}^{-3}$ . Let us note, that the inclusion of three-nucleon interactions does reduce  $m_n^*$ , and the reduction increases with density [12]. However, since we do not know exact values of  $m_n^*$ , used in Ref. [10], we cannot analyze the relative importance of  $m_n^*$  and in-medium corrections to the squared matrix element. We assume (Sec. IID) that the effect of the effective masses is more important. Notice, in addition, that the in-vacuum differential neutron-neutron scattering cross section in Ref. [10] (the solid line in their Fig. 3) seems underestimated.

In Fig. 4 we compare partial shear viscosities in a neutron star core with the APR EOS at  $T = 10^8 \text{ K}$ . Previously, it has been widely thought that  $\eta_n$  completely dominates over  $\eta_{e\mu}$  in the core of a nonsuperfluid star. Now we have considerably lowered both viscosities (Figs. 1 and 3). The main contribution to the total shear viscosity ( $\eta_{\text{tot}}$ , the solid line) at  $T = 10^8 \text{ K}$  comes from the electrons ( $\eta_e$ , the dashed line). The neutron viscosity  $\eta_n$  (the dash-dotted line) is lower than  $\eta_e$ . Note, however, that the relation between  $\eta_n$  and  $\eta_e$  is temperature-dependent; when  $T$  decreases,  $\eta_n$  becomes more important (see Fig. 5 and a discussion below). The dotted line in Fig. 4 shows the muon shear viscosity  $\eta_\mu$ . For  $T = 10^8 \text{ K}$ , it becomes comparable with  $\eta_n$  at  $\rho \gtrsim 7 \times 10^{14} \text{ g cm}^{-3}$ .

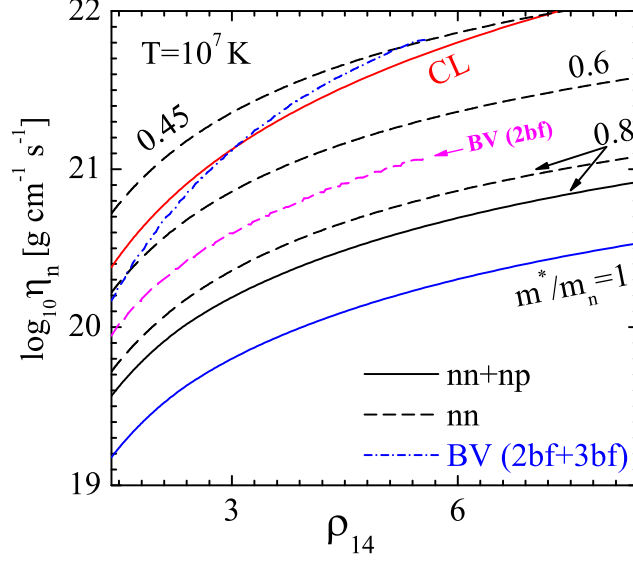


Figure 3: (Color online) Neutron shear viscosity versus  $\rho$  at  $T = 10^7$  K. The curve CL is the approximation of Cutler and Lindblom [2] of the results [6]. The curves BV (2bf) and BV (2bf+3bf) are obtained by Benhar and Valli [10] for pure neutron matter taking into account two-body and two-body plus three-body forces, respectively. Other curves are our results for the viscosity  $\eta_{nn}$ , limited by neutron-neutron collisions alone, or for the viscosity  $\eta_n$ , limited by neutron-neutron and neutron-proton collisions; these curves are calculated for the APR EOS assuming various phenomenological density independent effective masses  $m_n^*$  and  $m_p^*$ .

### C. Shear viscosity in superfluid matter

Now we discuss the shear viscosity in the presence of proton superfluidity (superconductivity) but for nonsuperfluid neutrons. For illustration, we take  $m_n^* = m_p^* = 0.8 m_n$  throughout a neutron star core.

Figure 5 demonstrates the temperature dependence of  $\eta_{e\mu}$  (solid lines) and  $\eta_n$  (dashed lines) in the presence of proton superfluid ( $T_{cp} = 10^9$  K, curves SF) and for non-superfluid matter (unmarked curves) at  $\rho = 4 \times 10^{14}$  g cm $^{-3}$ .

In a non-superfluid matter,  $\eta_{e\mu}$  exceeds  $\eta_n$  at  $T \gtrsim 10^7$  K (for the adopted values of  $m_n^*$  and  $m_p^*$ ) but the situation reverses at lower  $T$ . The reversal is a consequence of the different temperature behaviors,  $\eta_{e\mu} \propto T^{-5/3}$  [Eq. (37)] and  $\eta_n \propto T^{-2}$ . The thin solid line shows  $\eta_{e\mu}$  calculated taking into account the exchange of longitudinal plasmons alone. It demonstrates the standard Fermi-system behavior,  $\eta_{e\mu} \propto T^{-2}$ , and overestimates  $\eta_{e\mu}$ . At  $T = 10^9$  K the overestimation is small. It reaches a factor of  $\sim$  three at  $T = 10^8$  K, and exceeds one order of magnitude at  $T \lesssim 10^7$  K.

Proton superfluidity noticeably increases  $\eta_{e\mu}$  at  $T < T_{cp}$  and restores the Fermi-liquid temperature behavior,  $\eta_{e\mu} \propto T^{-2}$  [Eq. (85)]. The increase of  $\eta_n$  is not large because it comes from superfluid suppression of neutron-proton collisions which give a relatively small contribution to  $\eta_n$ . In the presence of proton superfluidity,  $\eta_{e\mu}$  completely dominates over  $\eta_n$ .

The electron shear viscosity in superfluid matter has recently been considered by Andersson et al. [7]. We have already discussed their approach in Sec. III A 2. For their EOS and superfluidity model, their results overestimate  $\eta_e$ , typically, by a factor of three in superfluid matter and by more than one order of magnitude in non-superfluid matter.

Figure 6 compares the shear viscosity  $\eta$  (left panel) with the bulk viscosity  $\zeta$  (right panel) determined by the direct and modified Urca processes in the core of a vibrating neutron star at  $T = 10^7, 10^8$ , and  $10^9$  K. The vibration frequency is set to be  $\omega = 10^4$  s $^{-1}$ ; these vibrations strongly affect  $\zeta$  but do not affect  $\eta$ . The bulk viscosity is calculated according to Refs. [33, 34]. The EOS is the same as in [33, 34] (PAL I with  $K_0 = 180$  MeV).

Note, that  $\eta$  decreases with growing  $T$ , while  $\zeta$  increases (e.g., Refs. [33, 34]). For  $T = 10^7$  K, the shear viscosity dominates in the entire stellar core, while for  $T = 10^8$  K the bulk viscosity  $\zeta$  in the inner core (where the direct Urca process is allowed, after the jump of  $\zeta$  in the right panel) becomes  $\sim 10$  times higher than  $\eta$ . For  $T = 10^9$  K, the bulk viscosity completely dominates in the entire core. The presence of proton superfluidity enhances  $\eta$  and suppresses  $\zeta$ . The dashed lines in the left and right panels of Fig. 6 show  $\eta$  and  $\zeta$ , respectively, in superfluid matter with  $T_{cp} = 10^9$  K.

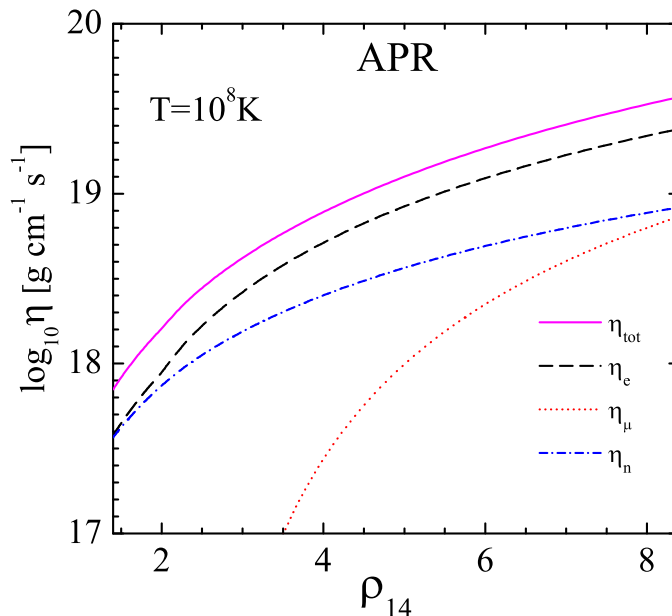


Figure 4: (Color online) Partial shear viscosities in non-superfluid neutron star cores versus density at  $T = 10^8$  K ( $m_n^* = m_p^* = 0.8m_n$ ).

at  $T = 10^8$  K. Superfluidity makes the shear viscosity more important. Note that shear perturbations in dense matter (e.g., associated with differential stellar rotation) are damped by the shear viscosity and can be unaffected by the bulk viscosity. Therefore, the shear viscosity can be important for applications even if it is lower than the bulk viscosity.

Finally, Fig. 7 compares the shear viscosity in the crust and the core of a neutron star. The viscosity in the crust is calculated for cold-catalyzed matter [1] using the results of Refs. [35] and [36]. The former paper is devoted to the viscosity mediated by electron-ion collisions, while Ref. [36] deals with the contribution of electron-electron collisions taking into account the exchange of transverse plasmons. In the crust, the latter effect is not large. We use the APR EOS in the core, and the core is assumed to be non-superfluid. The solid, dashed, and dash-dot lines correspond to  $T = 10^7$ ,  $10^8$ , and  $10^9$  K, respectively. The viscosity jump at the star crust-core interface (at  $\rho = 1.4 \times 10^{14}$  g cm $^{-3}$ ) is due to the disappearance of atomic nuclei in the core. The nuclei, present in the crust, lower the viscosity owing to a very efficient electron-ion scattering.

## V. CONCLUSIONS

We have calculated the shear viscosity in a neutron star core as a sum of the electron-muon viscosity  $\eta_{e\mu}$  and the neutron viscosity  $\eta_n$ . Calculating the viscosity  $\eta_{e\mu}$ , which is mediated by collisions of charged particles, we have taken into account the exchange of transverse plasmons (that has not been done before). Our results include also the effects of proton superfluidity. They are universal, presented in the form of analytic fit expressions convenient for implementing into computer codes for any EOS of nucleon matter in neutron star cores.

Our main conclusions are:

1. The exchange of transverse plasmons strongly reduces  $\eta_{e\mu}$  for all temperatures and densities of interest in a non-superfluid core. At low temperatures, we have  $\eta_{e\mu} \propto T^{-5/3}$ .
2. The viscosity  $\eta_{e\mu}$  generally dominates over  $\eta_n$ , although  $\eta_n$  can exceed  $\eta_{e\mu}$  at  $T \lesssim 10^7$  K and  $\rho \lesssim 4 \times 10^{14}$  g cm $^{-3}$  (for  $m_n^* \approx m_p^* \approx 0.8m_n$ ).
3. The viscosity  $\eta_n$  strongly depends on the nucleon effective masses. Typically, it is more than one order of magnitude lower, than that calculated in Ref. [6] and parametrized in Ref. [2].
4. Strong proton superfluidity significantly increases  $\eta_{e\mu}$  and restores its Fermi-liquid temperature dependence,  $\eta_{e\mu} \propto T^{-2}$ . In this regime,  $\eta_{e\mu}$  exceeds  $\eta_n$ .

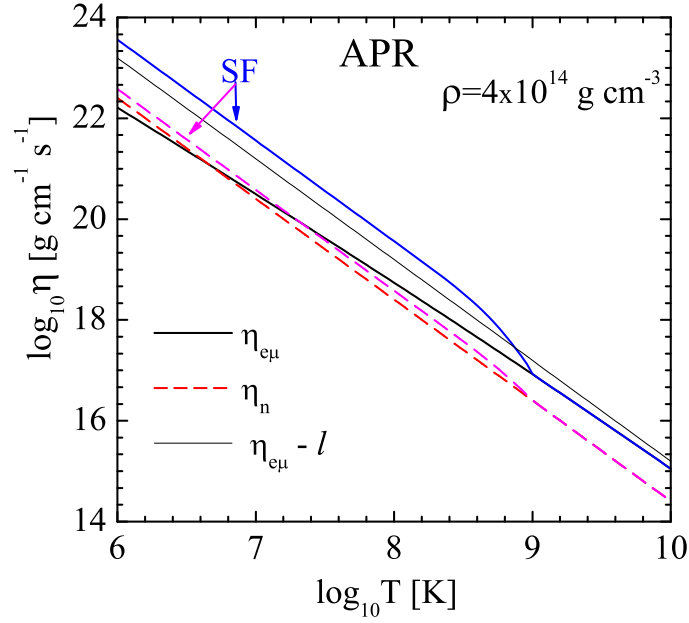


Figure 5: (Color online) Electron-muon and neutron shear viscosities versus temperature in the non-superfluid neutron star core and in the presence of proton superfluidity ( $T_{\text{cp}} = 10^9$  K) for the APR EOS at  $\rho = 4 \times 10^{14}$  g cm $^{-3}$  ( $m_n^* = m_p^* = 0.8m_n$ ). Curves SF correspond to the superfluid case, while other curves are for normal matter. The thin solid curve is  $\eta_{e\mu}$  calculated including the exchange of longitudinal plasmons alone.

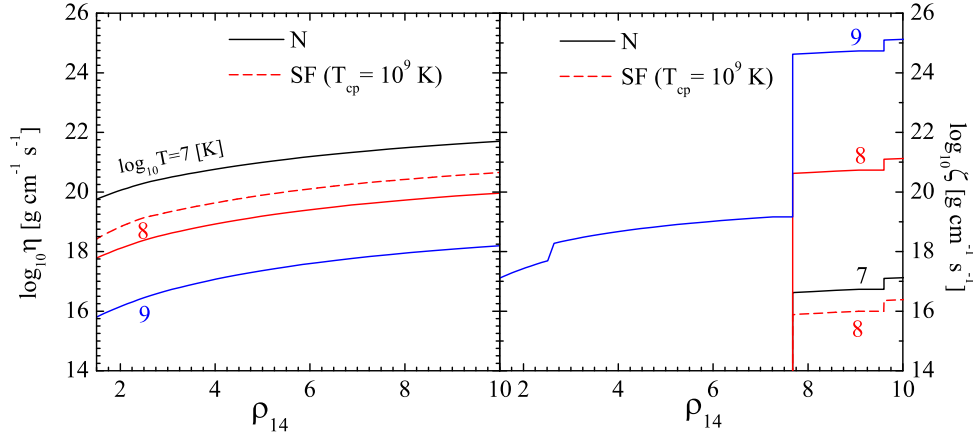


Figure 6: (Color online) Density dependence of the shear viscosity  $\eta$  (left) and the bulk viscosity  $\zeta$  (right) at different temperatures (the values of  $\log_{10} T$  are given near the curves) in a neutron star core with the PAL I EOS (see text). Solid curves are for normal matter (N). Dashed curves are for  $T = 10^8$  K and proton superfluidity with  $T_{\text{cp}} = 10^9$  K. The viscosity  $\zeta$  is plotted for a neutron star vibrating at a frequency of  $\omega = 10^4$  s $^{-1}$ .

5. The shear viscosity  $\eta$  is comparable with the bulk viscosity  $\zeta$  at  $T \sim 10^8$  K (for a star vibrating at a frequency  $\omega \sim 10^4$  s $^{-1}$ ) and dominates at lower  $T$ . Superfluidity increases the importance of  $\eta$  in comparison with  $\zeta$ .

Our results can be used in simulations of neutron star hydrodynamics, in particular, to analyze the damping of internal differential rotation, stellar oscillations, gravitational wave driving instabilities.

Our results can be improved further in many respects. It would be most important to study the shear viscosity problem in the presence of neutron and proton superfluidity in the frame of multifluid hydrodynamics as discussed in Sec. III.

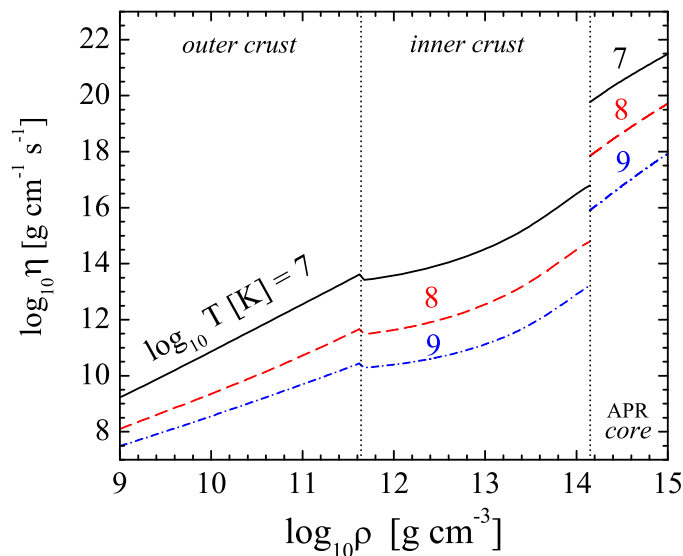


Figure 7: (Color online) Density profiles of the shear viscosity through a non-superfluid neutron star (through the outer crust, inner crust and the core) for three values of  $T$  ( $\log_{10} T$  [K] = 7, 8, and 9 – solid, dashed, and dash-dotted lines, respectively). The left vertical dotted line shows the neutron drip density, the right line is the crust-core interface.

Nevertheless, even our restricted standard one-fluid formulation is incomplete. Our calculations of  $\eta_n$  can be improved by taking into account the medium effects on the matrix elements of nucleon-nucleon scattering. However, we rely on the results of Ref. [12] that these medium effects are weaker than the effects of nucleon effective masses (which we include explicitly). An account for the medium effects on the matrix elements would complicate the expressions for  $\eta_n$  (making them non-universal).

We have also neglected the effects of strong magnetic field which can modify the shear viscosity. For not too high magnetic fields,  $B \lesssim 10^{13}$  G, which do not affect the plasma polarization functions (e.g., Ref. [37]), the generalization of the present results to the magnetic case is straightforward. For stronger fields, the polarization tensor becomes anisotropic and the viscosity problem is very complicated.

The present results are in line with our studies of kinetic properties of relativistic plasma taking into account the exchange of transverse plasmons. These effects were studied by Heiselberg and Pethick [8] for ultra-relativistic quark plasma. They should be included in all calculations of kinetic properties of relativistic plasmas, particularly in neutron stars. For the neutron star crust, the effect was studied in [38] (thermal conductivity) and [36] (shear viscosity). For neutron star cores, it was analyzed in [9] (thermal conductivity), [37] (electrical conductivity), and [39] (neutrino pair emission in electron-electron collisions).

### Acknowledgments

We are very grateful to U. Lombardo, A. I. Chugunov and D. A. Baiko for useful discussions and critical remarks. This work was partly supported by the Dynasty Foundation, by the Russian Foundation for Basic Research (grants 08-02-00837, 05-02-22003), and by the State Program “Leading Scientific Schools of Russian Federation” (grant NSH 2600.2008.2).

## Appendix A: EXPLICIT EXPRESSIONS FOR ANGULAR INTEGRALS

Here we present explicit expressions of the angular integrals  $I_k^{\parallel}(x)$ , defined by Eq. (40), for different values of  $k$ ,

$$I_0^{\parallel}(x) = \frac{1}{2} \arctan x + \frac{1}{2} \frac{x}{1+x^2}, \quad (\text{A1})$$

$$I_2^{\parallel}(x) = \frac{1}{2} \arctan x - \frac{1}{2} \frac{x}{1+x^2}, \quad (\text{A2})$$

$$I_4^{\parallel}(x) = x - \frac{3}{2} \arctan x + \frac{1}{2} \frac{x}{1+x^2}, \quad (\text{A3})$$

$$I_6^{\parallel}(x) = \frac{x^3}{3} - 2x + \frac{5}{2} \arctan x - \frac{1}{2} \frac{x}{1+x^2}, \quad (\text{A4})$$

$$I_8^{\parallel}(x) = \frac{x^5}{5} - \frac{2x^3}{3} + 3x - \frac{7}{2} \arctan x + \frac{1}{2} \frac{x}{1+x^2}. \quad (\text{A5})$$

- [1] P. Haensel, A. Y. Potekhin, and D. G. Yakovlev, *Neutron Stars. 1. Equation of State and Structure* (Springer, New York, 2007).
- [2] C. Cutler and L. Lindblom, *Astroph. J.* **314**, 234 (1987).
- [3] N. Andersson, D. I. Jones, K. D. Kokkotas, and N. Stergioulas, *Astrophys. J.* **534**, L75 (2000).
- [4] S.L. Shapiro and S.A. Teukolsky, *Black Holes, White Dwarfs, and Neutron Stars* (Wiley-Interscience, New York, 1983)
- [5] U. Lombardo and H.-J. Schulze in *Physics of Neutron Star Interiors*, edited by D. Blaschke, N. K. Glendenning, and A. Sedrakian (Springer, Berlin, 2001), p. 30.
- [6] E. Flowers, N. Itoh, *Astrophys. J.* **230**, 847 (1979).
- [7] N. Andersson, G. L. Comer, and K. Glampedakis, *Nucl. Phys. A* **763**, 212 (2005).
- [8] H. Heiselberg and C.J. Pethick, *Phys. Rev. D* **48**, 2916 (1993).
- [9] P.S. Shternin and D.G. Yakovlev, *Phys. Rev. D* **75**, 103004 (2007) – SY07.
- [10] O. Benhar and M. Valli, *Phys. Rav. Lett.* **2007**, 232501 (2007).
- [11] D. A. Baiko, P. Haensel, D. G. Yakovlev, *Astron. Astrophys.* **374**, 151 (2001) – BHY01.
- [12] H. F. Zhang, Z. H. Li, U. Lombardo, P. Y. Luo, F. Sammarruca, and W. Zuo, *Phys. Rev. C* **76**, 054001 (2007).
- [13] E. Flowers, N. Itoh, *Astrophys. J.* **206**, 218 (1976).
- [14] J. Sykes and G. A. Brooker, *Annals of Physics* **56** 1 (1970).
- [15] R. H. Anderson, C. J. Pethick, and K. F. Quader, *Phys. Rev. B* **35**, 1620 (1987).
- [16] D. A. Baiko and P. Haensel, *Acta Physica Polonica B* **30**, 1097 (1999).
- [17] G. Q. Li and R. Machleidt, *Phys. Rev. C* **48**, 1702 (1993).
- [18] G. Q. Li and R. Machleidt, *Phys. Rev. C* **49**, 566 (1994).
- [19] R. Machleidt, K. Holinde, and Ch. Elster, *Phys. Rep.* **149**, 1 (1987).
- [20] M. E. Gusakov, *Phys. Rev. D* **76**, 083001 (2007).
- [21] K. P. Levenfish and D. G. Yakovlev, *Astron. Rep.* **38**, 247 (1994).
- [22] P. I. Arseev, S. O. Loiko, and N. K. Fedorov, *Phys. — Usp.* **49**, 1 (2006).
- [23] D. C. Mattis and J. Bardeen, *Phys. Rev.* **111**, 412 (1958).
- [24] O. Y. Gnedin, D. G. Yakovlev, *Nucl. Phys. A* **582**, 697 (1995)
- [25] D. G. Yakovlev, K. P. Levenfish, and Yu. A. Shibano, *Phys. — Usp.* **42**, 737 (1999).
- [26] A. Akmal, V. R. Pandharipande, and D. G. Ravenhall, *Phys. Rev. C* **58**, 1804 (1998).
- [27] H. Heiselberg, and M. Hjorth-Jensen, *Astroph. J. Lett.* **525**, L45 (1999).
- [28] M. E. Gusakov, A. D. Kaminker, D. G. Yakovlev, and O. Y. Gnedin, *Mont. Not. Roy. Astron. Soc.* **363**, 555 (2005)
- [29] M. Prakash, T.L. Ainsworth, and J.M. Lattimer, *Phys. Rev. Lett.* **61**, 2518 (1988).
- [30] D. Page and J.H. Applegate, *Astrophys. J. Lett.* **394**, L17 (1992).
- [31] G. Baym, H. A. Bethe, and C. J. Pethick, *Nucl. Phys.* **175**, 225 (1971).
- [32] E. Flowers E. and N. Itoh, *Astrophys. J.* **250**, 750 (1981).
- [33] P. Haensel, K.P. Levenfish, and D.G. Yakovlev, *Astron. Astrophys.* **357**, 1157 (2000).
- [34] P. Haensel, K.P. Levenfish, and D.G. Yakovlev, *Astron. Astrophys.* **372**, 130 (2001).
- [35] A. I. Chugunov and D.G. Yakovlev, *Astron. Rep.* **49**, 724 (2005).
- [36] P.S. Shternin, *J. Phys. A* **41**, 205501 (2008).
- [37] P.S. Shternin, *Zurn. Eksper. Teor. Fiz.* **134**, 255 (2008).
- [38] P.S. Shternin and D.G. Yakovlev, *Phys. Rev. D* **74**, 043004 (2006).
- [39] P. Jaikumar, C. Gale, and D. Page, *Phys. Rev. D* **72**, 123004 (2005).